ISSN 0915-633X

NATIONAL INSTITUTE FOR FUSION SCIENCE

Self-sustained Turbulence and L-Mode Confinement in Toroidal Plasmas

K. Itoh, S.-I. Itoh, A. Fukuyama, M. Yagi and M. Azumi

(Received – Mar. 22, 1993)

NIFS-219 Apr. 1993

RESEARCH REPORT
NIFS Series

NAGOYA, JAPAN

Self-sustained Turbulence and L-Mode Confinement in Toroidal Plasmas

K. Itoh*, S.-I. Itoh**, A. Fukuyama†, M. Yagi†† and M. Azumi††

* National Institute for Fusion Science, Nagoya 464-01, Japan

** Institute for Applied Mechanics, Kyushu University 87, Kasuga 816, Japan

† Faculty of Engineering, Okayama University, Okayama 700, Japan

†† Japan Atomic Energy Research Institute, Naka, Ibaraki 311-01, Japan

Keywords: Anomalous transport, L-mode, Thermal conductivity, Current diffusivity, Ion viscosity, Nonlinear theory, Turbulence, Ballooning instability, Interchange instability, Magnetic shear, Magnetic well, Tokamak, Helical systems, Stellarators, Collisionless skin depth

Abstract

Theory of the L-mode confinement in toroidal plasmas is developed. The quantitative effect of the anomalous transport, which is caused by microscopic fluctuations, on the pressure-gradient- driven modes is analyzed. The E×B nonlinearity is renormalized in a form of the transport coefficient such as the thermal diffusivity, the ion viscosity and the current diffusivity. The destabilization by the current-diffusivity and the stabilization by the thermal transport and ion viscosity are analyzed. By use of the mean-field approximations, the nonlinear dispersion relation is solved. Growth rate and stability condition are expressed in terms of the renormalized transport coefficients. The transport coefficients in the steady state are obtained by the marginal stability condition for the least stable mode.

This method is applied to the microscopic ballooning mode for the toroidal plasma with the magnetic well (such as tokamak). The formula of the anomalous transport is obtained. The role of pressure gradient in enhancing the anomalous transport is identified. Effects of the geometrical parameters such as the rotational transform and magnetic shear are also quantified. The comparison with experimental observations are made. A good agreement is found in a various aspects of the L-mode plasmas; such as the power degradation of the confinement time, large transport coefficient at edge, ion mass effect and the favourable effect of the plasma current. The typical wavenumber and level of the fluctuations for the self-sustained turbulence is also

obtained. Important role of the collisionless skin depth is found.

The analysis is also made for the plasma with magnetic hill and shear (such as torsatron/Heliotron devices). This method is applied to the interchange modes. Formula of the anomalous transport is obtained. Also investigated is the case of the magnetic well and low magnetic shear (conventional stellarator). The roles of the pressure gradient and the collisionless skin depth in determining the anomalous transport are found to be generic in toroidal plasmas. The difference in the magnetic configuration affects the transport coefficient. These formula explain major experimental observations on the L-mode confinement in helical plasmas including the differences from tokamak experiments.

Contents

1. Introduction

The transport of the plasma across the magnetic field in tokamaks is much faster than that by Coulomb collisions. It has long been known as the anomalous transport (For a Review, see, for instance Liewer 1985). The L-mode confinement, in which the energy confinement time τ_E decreases as the heating power P is increased, is observed in almost all of the toroidal plasmas. The L-mode confinement is a generic feature of toroidal plasmas. A database has been constructed (Goldston 1984, Yushmanov et al. 1990) on how τ_E depends on the externally controllable parameters, such as P and the plasma current I_p. The radial profile of the effective thermal conductivity χ (the ratio of the energy flux per particle to the temperature gradient ∇T) has been studied. (For a review of present status, see, Houlberg et al. 1990, Wootton et al. 1990, Ross et al. 1991.) The ion viscosity is also enhanced, and is the same order of the electron and ion thermal conductivities (Burrell et al. 1988, Ida et al. 1991).

The paradigm to understand the transport phenomena is that the anomalous transport is caused by the microscopic instabilities (Liewer 1985). Theoretical development has been made based on the mixing length estimate (Kadomtsev 1965), the scale invariance method (Connor and Tayler 1977) or the one/two point renormalization methods (Dupree 1966, 1972). (These gave identical results from the view point of the physics argument (Yagi 1989).) The theories has shown, in general, that the

transport coefficient is larger for hotter plasmas, which is consistent with the power degradation of τ_E. It was also shown that the ion viscosity can also be enhanced to the level of the thermal transport diffusivity (Itoh 1992). These results have shown the progress of the theories. It has been confirmed, experimentally, that the microscopic fluctuations play important roles for the anomalous transport process (Wootton et al. 1990, Ross et al. 1991). However, the experiments have shown that χ-value is increasing towards the edge while the plasma temperature is becoming lower. This fact is in contrast to what have been predicted by theories. The Ohkawa's model (Ohkawa 1978), based on fluctuations of the scale length of the collisionless skin depth δ, is one of the few which can explain that the χ-value is larger near the edge and that χ is an increasing function of the temperature. But it does not fully explain the dependences of τ_E. No theory has succeeded in explaining the radial shape of χ and the scaling $\tau_E[P, I_p, \cdots]$ simultaneously (For a review, see for instance Callen 1992). The understanding of the L-mode plasma is far from satisfactory.

We have recently reported a new theory to determine the transport coefficient which is enhanced by the pressure gradient itself (Itoh et al. 1992a, 1992b, 1993). In this new approach, we incorporate the effects of the anomalous transport process on the mode stability itself. (The magnetic shear-stabilized plasma can become unstable due to the fluctuation-driven dissipation, and the analysis on the self-sustaining turbulence has been developed (Hirshman and Molvig 1979, Scott 1990, Itoh et al.

1992a, 1992b, 1993, Wakatani et al. 1992.) It is found that, below the beta-limit of the ideal magnetohydrodynamic (MHD) mode, the microscopic ballooning mode can be unstable if there is the plasma transport such as the current-diffusivity λ, and that other transport coefficients, χ, and the ion viscosity μ, stabilize the mode (Itoh et al. 1992a, 1992b, 1993). The transport coefficients are determined by the marginal stability condition for the least stable mode. This results on the selfconsistent treatment of the anomalous transport was confirmed by the scale invariance method (Connor 1993).

In this article, we develop the nonlinear theory for the microscopic, pressure-driven instability, by keeping the E×B nonlinearity. The nonlinear interactions are renormalized in a form of the diffusion effects on the mode. By using the mean-field approximation, the renormalized transport coefficients are obtained. The eigenmode equation, which includes the nonlinear interactions in a form of transport coefficients, are solved. The toroidal geometry and the effects of magnetic shear and well/hill are taken into account. The nonlinear growth rate and mode structure are obtained. It is found that the mode (i.e., the microscopic ballooning mode in tokamak geometry) is destabilized by the current diffusivity, and is stabilized by μ and χ. These transport coefficients are enhanced by the nonlinear interactions. The (de)stabilizing effects depend on the magnitude of the fluctuations. When the fluctuation level is low, the destabilizing effect is stronger than the stabilizing effects on turbulence itself. At a certain level of fluctuation

amplitude, the balance of destabilizing and stabilizing effects takes place, and the stationary state is realized. The marginal stability condition is thus realized. From the marginal stability condition of the least stable mode, the anomalous transport coefficient and the fluctuation level are simultaneously given.

This method is firstly applied to tokamak plasmas. The explicit form of χ due to the ballooning mode in tokamaks is obtained. Then the plasma with the magnetic shear and magnetic hill (such as torsatron/heliotron devices (Gouldon et al. 1968, Mohri et al. 1970a 1970b, Uo 1971) is analyzed. Finally, the transport coefficient is discussed for the plasma with magnetic well and very weak shear (conventional $\bar{\ell}=2$ stellarator; $\bar{\ell}$ is the multipolarity of the helical field). The anomalous transport is shown to be intrinsically dependent on the geometry and the plasma profile. The theoretical result of χ is compared to the experimental observations on the L-mode plasma, where the key feature of the toroidal confinement is considered. The agreements are shown. In low temperature limit, the resistivity takes over the driving mechanism from the current diffusivity. This corresponds to the change from the Pseudo-classical confinement (Yoshikawa 1970) to the L-mode confinement in low temperature plasmas.

The constitution of this article is as follows. In section 2, the model equation is derived. The renormalization process and assumptions are discussed. In §3, the set of model equations, which include the nonlinear effects in a form of

diffusion effects, is solved for tokamak plasmas. The marginal stability condition is derived. In §4, the transport coefficients are derived. The typical wave number and the level of the fluctuations are also described. The comparison with experimental observations on tokamak L-mode is given in §5. The analysis on the torsatron/Heliotron plasmas and the comparison with experiments are given in §6. Transport coefficient in conventional stellarator is discussed in §7. Summary and discussions are given in §8. Change from Pseudo-classical confinement to the L-mode is briefly discussed. Appendix A is devoted to the expression of the transport matrix. The theory in the main text is developed on the assumption that the background fluctuations are isotropic in the directions which are perpendicular to the magnetic field. The extension to the case of anisotropic turbulence is given in Appendix B.

2. Model Equation

2.1 Basic Equation

We study the circular tokamak with the toroidal coordinates (r, θ, ζ). The reduced set of equations (Strauss 1977) is employed. The equation of motion:

$$n_i m_i \{d(\nabla_\perp^2 \phi)/dt - \mu_c \nabla_\perp^4 \phi\} = B^2 \nabla_{/\!/} J + B\{\nabla p \times \nabla(2r\cos\theta/R)\}\cdot\zeta \quad (1)$$

The Ohm's law:

$$E + v \times B = \frac{1}{\sigma_c} J - \lambda_c \nabla_\perp^2 J - \frac{m_e}{ne^2} \frac{d}{dt} J \quad (2)$$

and the energy balance equation

$$dp/dt = \chi_c \nabla_\perp^2 p \quad (3)$$

constitute the set of basic equations. In these equations following notations are used: m_i is the ion mass, n_i is the ion density, m_e is the electron density, E is the electric field, B is the main magnetic field, p is the plasma pressure, and J is the current. The transport coefficients due to the Coulomb collisions are kept and denoted by the suffix c (the current-diffusivity λ, the thermal diffusivity χ, the ion viscosity μ,

and σ is the conductivity). ϕ is the stream function, and the velocity is given as

$$v = -\nabla\phi\times\vec{b}/B \tag{4}$$

where $\vec{b}$ is the unit vector in the direction of the main magnetic field. The time derivative of the quantity Y, dY/dt, is given as

$$dY/dt = \partial Y/\partial t + [\phi, Y]/B \tag{5}$$

where the bracket [] denotes the Poisson's bracket:

$$[f, g] = (\nabla f\times\nabla g)\cdot\vec{b} \tag{6}$$

This bracket represents the E×B nonlinearity. We keep the finite electron mass effect in the Ohm's law, in order to study the influence of the current diffusion which causes the collisionless reconnection (Ohkawa 1978).

2.2 Derivation and Assumptions of the Model Equation

In the following, we simplify the basic equation by the renormalization of the turbulence. We here overview the procedure and list the approximations and assumptions for the derivation of the model equations.

First, we solve the process of the excitation of the driven mode (k_2) by the interaction of the test mode (k) and the back-

ground turbulence (k_1). [The process $k+k_1 \rightarrow k_2$.] We then calculate the back reaction of the driven mode to the test mode through the interaction of the back-ground fluctuations. [The process $k_2+(-k_1) \rightarrow k$.] By this procedure, the test wave equation is derived by keeping the nonlinear contributions of the back-groung fluctuations. (One point renormalization.) By this procedure, the nonlinear term is treated as the effective diffusion on the test waves. For the simplicity, we in this article only keep the diagonal term in the diffusion-driven-transport effects on the test wave. We take the assumption that the back-ground fluctuation is isotropic. We finally employ the mean-field approximation, by which the nonlinear contributions are characterized into the three scalar parameters.

2.3 Renormalization

The nonlinear equations (1)-(3) are transformed to the model equation by employing the renormalization. In the process of the renormalization, we keep the process of the back-interaction of the driven modes (characterized by k_2) to the original test mode (denoted by k). In this renormalization, we study the E×B nonlinearlity. This is because we are interested in the anomalous transport driven by the electric fluctuations. (The renormalization is also possible for the case of the magnetic turbulence (Lichtenberg et al. 1992). The analysis will be reported in a separate article: The result is summarized in a same form of the renormalized equation with different coefficients.)

The equation for the driven mode is derived from Eqs.(1)-(3) in the electrostatic limit as

$$\left(\frac{\partial}{\partial t}+\Gamma_{u2}\right)U_2 - A_2 p_2 - igk_{//2}J_2 = -\frac{1}{B}[\Phi_1, \tilde{U}] \tag{7}$$

$$\left(\frac{\partial}{\partial t}+\Gamma_{j2}\right)J_2 + i\xi k_{//2}\Phi_2 = -\frac{1}{B}[\Phi_1, \tilde{J}] \tag{8}$$

and

$$\left(\frac{\partial}{\partial t}+\Gamma_{p2}\right)p_2 + \frac{1}{B}[\Phi_2, p_0] = -\frac{1}{B}[\Phi_1, \tilde{p}] \tag{9}$$

where $U \equiv \nabla_\perp^2\Phi$, and the suffix 1 indicates the background fluctuations, 2 indicates the driven mode with k_2, and 0 indicates the equilibrium profile, respectively. Classical collision term is neglected in Eqs.(7)-(9). Notations Γ_{u2}, Γ_{j2} and Γ_{p2} denote the decorrelation rates of U_2, J_2 and p_2 by the back-ground turbulence, respectively. The symbol ~ denotes the test wave. The coefficients g and ξ and the operator A are introduced to simplify the notation as

$$g \equiv B^2/m_i n_i \tag{10}$$

$$\xi = n_e e^2/m_e \tag{11}$$

and

$$Ap \equiv \frac{B}{m_i n_i}\left[\nabla \frac{2r\cos\theta}{R} \times \hat{\zeta}\right] \cdot \nabla p \qquad (12)$$

Components (U_2, J_2, p_2) are solved in terms of $[\Phi_1, \tilde{U}]$, $[\Phi_1, \tilde{J}]$, and $[\Phi_1, \tilde{p}]$ as

$$U_2 = \frac{1}{K_2}\left[k_{2\perp}{}^2 N_1 + \frac{i k_{2/\!/} g k_{2\perp}{}^2}{\tau_{j2}} N_2 + \frac{A_2 k_{2\perp}{}^2}{\tau_{p2}} N_3 \right] \qquad (13)$$

$$J_2 = \frac{1}{K_2}\left[\frac{\tau_{u2}}{\tau_{j2}}\left[k_{2\perp}{}^2 + \frac{i A_2 k_{2\theta} \nabla p_0}{\tau_{u2}\tau_{p2} B}\right] N_2 + \frac{i k_{2/\!/}\xi}{\tau_{j2}}\left[N_1 + \frac{A_2}{\tau_{p2}} N_3\right] \right] \qquad (14)$$

and

$$p_2 = \frac{1}{K_2}\left[\frac{\tau_{u2}}{\tau_{p2}}\left[k_{2\perp}{}^2 + \frac{g\xi k_{2/\!/}{}^2}{\tau_{u2}\tau_{j2}}\right] N_3 - \frac{i k_{2\theta} \nabla p_0}{\tau_{p2} B}\left[N_1 + \frac{i g k_{2/\!/}}{\tau_{j2}} N_2\right] \right] \qquad (15)$$

where

$$K_2 = \tau_{u2} k_{2\perp}{}^2 + g\xi \frac{k_{2/\!/}{}^2}{\tau_{j2}} + \frac{i A_2 k_{2\theta} \nabla p_0}{\tau_{p2}\, B} \qquad (16)$$

$\tau_{u2}=\tau(2)+\Gamma_{u2}$, $\tau_{j2}=\tau(2)+\Gamma_{j2}$, $\tau_{p2}=\tau(2)+\Gamma_{p2}$, $\tau(2)$ is the eigenvalue of the k_2 mode, $\partial\{U_2, J_2, p_2\}/\partial t = \tau(2)\{U_2, J_2, p_2\}$, and nonlinear terms $N_{1,2,3}$ are defined as

$$N_1 = - \frac{1}{B} [\Phi_1, \tilde{U}] \tag{17}$$

$$N_2 = - \frac{1}{B} [\Phi_1, \tilde{J}] \tag{18}$$

and

$$N_3 = - \frac{1}{B} [\Phi_1, \tilde{p}]. \tag{19}$$

The terms N_1 in the right hand side of Eq.(14), N_2 in Eq.(15) and N_3 in Eq.(16) are the diagonal terms, respectively, and others are the off-diagonal terms in the transport process.

The equation of the test wave is given from Eqs.(1)-(3), by keeping the back interaction of the driven mode, as

$$\frac{\partial}{\partial t} \tilde{U} - g \nabla_{//} \tilde{J} - A \tilde{p} = N_U \tag{20}$$

$$\frac{\partial}{\partial t} \tilde{\Psi} + \nabla_{//} \tilde{\Phi} + \frac{1}{\sigma} \tilde{J} = N_J \tag{21}$$

and

$$\frac{\partial}{\partial t}\tilde{p} + \frac{1}{B}[\tilde{\Phi}, p_0] = N_p \tag{22}$$

where $\mu_0 J = -\nabla_\perp^2 \psi$, and the nonlinear terms are given as

$$N_U = -\frac{1}{B}\Sigma\,[\Phi_{-1}, U_2] \tag{23}$$

$$N_J = -\frac{m_e}{n_e e^2}\frac{1}{B}\Sigma\,[\Phi_{-1}, J_2] \tag{24}$$

$$N_p = -\frac{1}{B}\Sigma\,[\Phi_{-1}, p_2] \tag{25}$$

and the suffix -1 indicates the modes of $-k_1$, and summation is taken over k_1.

Substituting Eqs.(13)-(15) into Eqs.(23)-(25), the renormalized set of equation is obtained.

2.4 Diffusion Matrix and Diagonal Approximation

The nonlinear terms (23)-(25) can be expressed in the matrix form, because $\{U_2, J_2, p_2\}$ are given in the form of the linear combination of $\{N_1, N_2, N_3\}$. We write

$$\begin{pmatrix} \mathcal{N}_U \\ \mathcal{N}_J \\ \mathcal{N}_p \end{pmatrix} = \frac{1}{B^2} \Sigma \begin{pmatrix} H_{11} & H_{11} & H_{13} \\ H_{21} & H_{22} & H_{23} \\ H_{31} & H_{32} & H_{33} \end{pmatrix} \begin{pmatrix} [\Phi_{-1}, [\Phi_1, \tilde{U}]] \\ [\Phi_{-1}, [\Phi_1, \tilde{J}]] \\ [\Phi_{-1}, [\Phi_1, \tilde{p}]] \end{pmatrix} \qquad (26)$$

where summation is taken over k_1. The matrix elements H_{ij} are given directly from Eqs.(13)-(16) and the explicit form is given in the appendix A.

The nonlinear operator $[\Phi_{-1}, [\Phi_1, \tilde{Y}]]$ is explicitly written as

$$[\Phi_{-1}, [\Phi_1, \tilde{Y}]] = \left(\left|\frac{\partial \Phi_1}{\partial x}\right|^2 \frac{\partial^2}{\partial y^2} + \left|\frac{\partial \Phi_1}{\partial y}\right|^2 \frac{\partial^2}{\partial x^2} \right) \tilde{Y}$$

$$+ \left(i k_{1y} \frac{\partial}{\partial x} \{ \Phi_{-1} \frac{\partial}{\partial x} \Phi_1 \} \right) \frac{\partial}{\partial y} \tilde{Y}$$

$$- \left(k_{1y}{}^2 \frac{\partial}{\partial x} \{ \Phi_{-1} \Phi_1 \} \right) \frac{\partial}{\partial x} \tilde{Y}$$

$$- \left(i k_{1y} \{ \Phi_1 \frac{\partial}{\partial x} \Phi_{-1} - \Phi_{-1} \frac{\partial}{\partial x} \Phi_1 \} \right) \frac{\partial^2}{\partial x \partial y} \tilde{Y} \qquad (27)$$

where x is taken in the radial direction and y is in the poloidal direction. When the envelop of the background turbulence is almost uniform in space i.e.,

$$|k_1| >> \frac{|\nabla_x [\Sigma |\Phi_1|^2]|}{[\Sigma |\Phi_1|^2]} \qquad (28)$$

the term proportional to $\partial\tilde{Y}/\partial x$ is neglected. When the convective damping of the wave is not important, i.e.,

$$\left| \Phi_1 \frac{\partial \Phi_{-1}}{\partial x} - \Phi_{-1} \frac{\partial \Phi_1}{\partial x} \right| \ll |k_1 \Phi_1 \Phi_{-1}|, \tag{29}$$

the terms $\partial\tilde{Y}/\partial y$ and $\partial^2\tilde{Y}/\partial x \partial y$ are neglected. The nonlinear term is approximated as

$$[\Phi_{-1}, [\Phi_1, \tilde{Y}]] = \left(\left|\frac{\partial \Phi_1}{\partial x}\right|^2 \frac{\partial^2}{\partial y^2} + \left|\frac{\partial \Phi_1}{\partial y}\right|^2 \frac{\partial^2}{\partial x^2} \right) \tilde{Y} \tag{30}$$

We employ the assumption of the isotropic turbulence, i.e.,

$$|\partial \Phi_1 / \partial x|^2 \simeq |\partial \Phi_1 / \partial y|^2 \simeq |k_{1\perp} \Phi_1|^2 / 2. \tag{31}$$

By this assumption, Eq.(26) reduces to the diffusion form

$$\begin{pmatrix} N_U \\ N_J \\ N_p \end{pmatrix} = \Sigma \frac{|k_{1\perp} \Phi_1|^2}{2B^2} \begin{pmatrix} H_{11} & H_{11} & H_{13} \\ H_{21} & H_{22} & H_{23} \\ H_{31} & H_{32} & H_{33} \end{pmatrix} \nabla_\perp^2 \begin{pmatrix} \tilde{U} \\ \tilde{J} \\ \tilde{p} \end{pmatrix} \tag{32}$$

The nonlinear interaction is now renormalized in the form of the turbulent-driven transport coefficient for the test wave.

For the simplicity of the argument, only the diagonal

elements are kept in the following analysis. We write

$$N_U = \mu_k \nabla_\perp^2 \tilde{U} \tag{33}$$

$$N_J = \lambda_k \nabla_\perp^2 \tilde{J} \tag{34}$$

and

$$N_p = \chi_k \nabla_\perp^2 \tilde{p} \tag{35}$$

where the effective ion diffusivity, μ_k, effective current diffusivity, λ_k, and effective thermal diffusivity, χ_k, are defined as

$$\mu_k = \Sigma \frac{|k_{1\perp}\Phi_1|^2}{2B^2} \frac{k_{2\perp}^2}{K_2} \tag{36}$$

$$\lambda_k = \delta^2 \mu_0 \mu_{ek} \tag{37-1}$$

$$\mu_{ek} = \Sigma \frac{|k_{1\perp}\Phi_1|^2}{2B^2} \frac{1}{K_2} \frac{\tau_{u2}}{\tau_{j2}} \left[k_{2\perp}^2 + \frac{iA_2 k_{2\theta} \nabla p_0}{\tau_{u2}\tau_{p2}B} \right] \tag{37-2}$$

$$\chi_k = \Sigma \frac{|k_{1\perp}\Phi_1|^2}{2B^2} \frac{1}{K_2} \frac{\tau_{u2}}{\tau_{p2}} \left[k_{2\perp}^2 + \frac{g\xi k_{2/\!/}^2}{\tau_{u2}\tau_{j2}} \right] \tag{38}$$

μ_e denotes the electron viscosity, and δ is the collisionless skin depth

$$\delta = c/\omega_p \qquad (39)$$

(ω_p;electron plasma frequency). The suffix k indicates that the right hand side of Eqs.(36)-(38) can be dependent on the choice of the test wave. The decorrelation rates of the driven mode, Γ_{u2}, Γ_{j2} and Γ_{p2} are also given by the diffusion operator and are evaluated as $\mu_{k2}k_{2\perp}^2$, $\mu_{ek2}k_{2\perp}^2$ and $\chi_{k2}k_{2\perp}^2$, respectively.

2.5 Mean-Field Approximation and Model Set of Equations

The original nonlinear equations are reduced to a coupled equations with the transport coefficients, $\{\mu_k, \lambda_k, \chi_k\}$. The purpose of this study is to obtain the level of the anomalous transport, not to obtain the precise form of the turbulent spectrum. We therefore take the mean-filed approximation to obtain the analytic insight of the problem.

The mean-field approximation is to characterize the nonlinear interactions on the different modes by a single set of constants, which are independent on the wave number of the test mode. We approximate the constants $\{\mu_k, \lambda_k, \chi_k\}$ by a set of diffusion coefficients $\{\mu, \lambda, \chi\}$. As is discussed in Horton (1984), quantities which are defined by Eqs.(36)-(38) reduce to the diffusion constants in the range of the long wave length. Since the range of k_2 is similar to that of k_1, we approximate as

$$\mu_k = \mu, \qquad (40)$$

$$\lambda_k = \lambda, \tag{41}$$

$$\chi_k = \chi \tag{42}$$

The transport coefficients $\{\mu, \lambda, \chi\}$ are calculated as

$$\mu = \Sigma \frac{|k_{l\perp}\Phi_l|^2}{2B^2} \frac{k_{l\perp}^2}{K_l} \tag{43}$$

$$\lambda = \delta^2 \mu_0 \mu_e \tag{44-1}$$

$$\mu_e = \Sigma \frac{|k_{l\perp}\Phi_l|^2}{2B^2} \frac{1}{K_l} \frac{\tau_{ul}}{\tau_{jl}} \left(k_{l\perp}^2 + \frac{iA_l k_{l\theta} \nabla p_0}{\tau_{ul}\tau_{pl} B} \right) \tag{44-2}$$

and

$$\chi = \Sigma \frac{|k_{l\perp}\Phi_l|^2}{2B^2} \frac{1}{K_l} \frac{\tau_{ul}}{\tau_{pl}} \left(k_{l\perp}^2 + \frac{g\xi k_{l/\!/}^2}{\tau_{ul}\tau_{jl}} \right) \tag{45}$$

where

$$K_l = \tau_{ul} k_{l\perp}^2 + g\xi \frac{k_{l/\!/}^2}{\tau_{jl}} + \frac{iA_l k_{l\theta} \nabla p_0}{\tau_{pl} B} \tag{46}$$

$\tau_{ul} = \tau(1) + \mu k_{l\perp}^2$, $\tau_{jl} = \tau(1) + \mu_e k_{l\perp}^2$, $\tau_{pl} = \tau(1) + \chi k_{l\perp}^2$, and $\tau(1)$

is defined by $\partial Y_I/\partial t = \tau(1)Y_I$. $\{\mu, \lambda, \chi\}$ are the sum of the classical terms, $\{\mu_C, \lambda_C, \chi_C\}$, and the terms in Eqs.(43)-(45).

Combining these procedures, we have the set of model equations for the nonlinear waves driven by the pressure gradient in the following form.

Equation of motion:

$$n_i m_i \{\partial(\nabla_\perp^2\phi)/\partial t - \mu\nabla_\perp^4\phi\} = B^2\nabla_{/\!/} J + B\nabla p\times\nabla(2r\cos\theta/R)\cdot\hat{\zeta} \quad (47)$$

The Ohm's law:

$$E+v\times B = \frac{1}{\sigma} J - \lambda\nabla_\perp^2 J \quad (48)$$

and the energy balance equation

$$\frac{\partial}{\partial t} p + \frac{1}{B}[\phi, p_0] = \chi\nabla_\perp^2 p \quad (49)$$

where the tilde denoting the test wave is suppressed.

3. Solution of the Dispersion Relation for Tokamaks

3.1 Ballooning Transformation

Figure 1 illustrates the geometry of the plasma. The ballooning transformation is employed as (Connor et al. 1979)

$$\phi(r,\theta,\zeta)=\sum_m \exp(-im\theta+in\zeta)\int\phi(\eta)\exp\{im\eta-inq\eta\}d\eta, \qquad (50)$$

(q is the safety factor) since we are interested in the microscopic modes. The partial differential equation is reduced to the ordinary differential equation as (Yagi et al. 1993)

$$\frac{d}{d\eta}\frac{F}{\hat{\tau}+\Xi F+\Lambda F^2}\frac{d\phi}{d\eta}+\frac{\alpha[\kappa+\cos\eta+(s\eta-\alpha\sin\eta)\sin\eta]\phi}{\hat{\tau}+XF}$$

$$-(\hat{\tau}+MF)F\phi=0. \qquad (51)$$

In writing Eq.(51), we use the normalizations

$$r/a \rightarrow \hat{r}, \qquad (52\text{-}1)$$

$$t/\tau_{Ap} \rightarrow \hat{t}, \qquad (52\text{-}2)$$

$$\chi\tau_{Ap}/a^2 \rightarrow \hat{\chi}, \qquad (52\text{-}3)$$

$$\mu\tau_{Ap}/a^2 \rightarrow \hat{\mu}, \tag{52-4}$$

$$\tau_{Ap}/\mu_0\sigma_c a^2 \rightarrow 1/\hat{\sigma}, \tag{52-5}$$

$$\lambda\tau_{Ap}/\mu_0 a^4 \rightarrow \hat{\lambda}, \tag{52-6}$$

$$\tau\tau_{Ap} \rightarrow \hat{\tau}. \tag{52-7}$$

and use the notations

$$\tau_{Ap} \equiv a\sqrt{\mu_0 m_i n_i}/B_p, \tag{53-1}$$

$$\Xi = n^2q^2/\hat{\sigma}, \tag{53-2}$$

$$\Lambda = \hat{\lambda}n^4q^4, \tag{53-3}$$

$$\Upsilon = \hat{\chi}n^2q^2, \tag{53-4}$$

$$M = \hat{\mu}n^2q^2. \tag{53-5}$$

Other notations are standard: $B_p=Br/qR$, $\varepsilon=r/R$, a and R are the major and minor radii, β is the pressure divided by the magnetic pressure ($\beta=\mu_0 n(T_e+T_i)/B^2$), τ is the growth rate, s is the shear parameter,

$$s = r(dq/dr)/q, \tag{54-1}$$

$$F=1+(s\eta-\alpha\sin\eta)^2, \tag{54-2}$$

κ is the average well,

$$\kappa\equiv-(r/R)(1-1/q^2), \tag{54-3}$$

α denotes the normalized pressure gradient,

$$\alpha=q^2\beta'/\varepsilon \tag{54-4}$$

and $\beta'\equiv d\beta/d\hat{r}$.

The partial differential equation is reduced to the ordinary differential equation, Eq.(51). This equation is the generalization of the previous ballooning equations (Connor et al. 1979). If we neglect $\hat{\lambda}$, $\hat{\imath}$ and $\hat{\mu}$, Eq.(51) is reduced to the resistive ballooning equation as

$$\frac{d}{d\eta}\frac{\hat{\gamma}F}{\hat{\gamma}+\Xi F}\frac{d\phi}{d\eta}+\alpha[\kappa+\cos\eta+(s\eta-\alpha\sin\eta)\sin\eta]\phi-\hat{\gamma}^2F\phi=0 \tag{55}$$

The ideal MHD mode equation is recovered by further taking $1/\hat{\sigma}=0$ ($\Xi=0$) as

$$\frac{d}{d\eta}F\frac{d\phi}{d\eta}+\alpha[\kappa+\cos\eta+(s\eta-\alpha\sin\eta)\sin\eta]\phi-\hat{\gamma}^2F\phi=0 \tag{56}$$

3.2 Current-Diffusive Instability

We here review the stability analysis briefly. Details are given in Yagi et al. (1993). Since κ is small but is negative, the interchange mode is stable and the ballooning mode is the most unstable. Equation (51) predicts that the current-diffusive ballooning mode has a large growth rate. We take the limit of $1/\hat{\sigma}=0$. (The validity of this simplification is discussed in the final section.) The growth rate of the short wave length mode, driven by the $\hat{\Lambda}$ term, is estimated by the Wentzel-Kramers-Brillouin (WKB) method by neglecting $\hat{\chi}$ and $\hat{\mu}$ terms. For the most unstable mode, we have

$$\frac{\pi}{4} = \int_0^{\eta_c} d\eta \sqrt{\frac{1+\Lambda F^2/\hat{\tau}}{F}} \sqrt{\alpha\{\cos\eta-(s\eta-\alpha\sin\eta)\sin\eta\}-\hat{\tau}^2 F} \qquad (57)$$

where the kernel of the integral vanishes at $\eta=\eta_c$ and the well term κ is neglected. For the analytic insight, we take the short wave length limit, $\Lambda/\hat{\tau}>>1$, which yields

$$\sqrt{1/F+\Lambda F/\hat{\tau}} \simeq \sqrt{\Lambda F/\hat{\tau}}. \qquad (58)$$

By approximating $dF/d\eta \simeq 2s\sqrt{F}$, Eq.(57) is reduced to

$$\pi/4 \simeq [\sqrt{\Lambda/\hat{\tau}}/2s]\sqrt{\alpha}F_c, \qquad (59)$$

where $F_c = F(\eta_c)$. We also consider the case that the inertia term

determines η_c, having the estimate $F_c = \alpha/\hat{\tau}^2$. Using these limiting approximations, the dispersion relation Eq.(57) is written as

$$\pi/4 = [\sqrt{\Lambda/\hat{\tau}}/2s]\alpha^{3/2}/\hat{\tau}^2, \tag{60}$$

or (Itoh et al. 1992b)

$$\hat{\tau} \simeq \hat{\lambda}^{1/5}(nq)^{4/5}\alpha^{3/5}s^{-2/5}. \tag{61}$$

Since the exponent to λ is 1/5, even the very small current diffusivity gives rise to the ballooning instability. The condition $\Lambda/\hat{\tau} >> 1$ requires $\hat{\lambda} n^4 q^4 > \alpha^{3/4}/\sqrt{s}$.

This large growth rate is confirmed for a wide range of parameters by the numerical calculation (Yagi et al. 1993). Figure 2 illustrates α vs $\hat{\tau}$ and $\hat{\lambda}$ vs $\hat{\tau}$, keeping $\hat{\lambda}/\hat{\chi}$ and $\hat{\chi}/\hat{\mu}$ constant. The analytic estimation for small $\hat{\lambda}$ is confirmed. As the transport coefficients are increased much, the stabilizing effects by $\hat{\chi}$ and $\hat{\mu}$ overcome the destabilizing effect of $\hat{\lambda}$.

3.3 Marginal Stability Condition

The stability boundary is derived. Setting $\hat{\tau}=0$ in Eq.(51), we have the eigenvalue equation, which determines the relation between $\hat{\chi}$, $\hat{\lambda}$ and $\hat{\mu}$. We here study the case that the ballooning mode is destabilized by the normal curvature, not by the geodesic curvature, i.e.,

$$1/2+\alpha > s. \qquad (62)$$

For the strongly localized mode, $s^2\eta^2<1$ and $\eta^2<1$, this eigenvalue equation is approximated by the Weber type equation as

$$d^2\phi/d\eta^2 + (\alpha\hat{\lambda}n^2q^2/\hat{\chi})\{1-(1/2+\alpha-s)\eta^2\}\phi$$

$$- \hat{\mu}\hat{\lambda}n^6q^6(1+3s^2\eta^2)\phi = 0. \qquad (63)$$

This equation gives the marginal stability condition, which then yields the constraint between the plasma pressure gradient and the fluctuation induced transport coefficients, as

$$\alpha^{3/2}\hat{\lambda}\hat{\chi}^{-3/2}\hat{\mu}^{-1/2} = f_1(N) \qquad (64)$$

$$f_1(N) \equiv N^{-2}(1-N^4)^{-2}\{(1/2+\alpha-s)+3s^2N^4\} \qquad (65)$$

The normalized mode number N is defined as

$$N=nq(\hat{\chi}\hat{\mu}/\alpha)^{1/4}. \qquad (66)$$

This analytic result is confirmed by the numerical computation as is shown in Fig.3.

From Eq.(63), the eigenmode structure of the Gaussian form is expressed as

$$\phi(\eta) = \exp\{-(\eta/\eta_0)^2\} \tag{67}$$

with

$$2\eta_0^{-2} = \alpha^{3/2}\hat{\lambda}\hat{\chi}^{-3/2}\hat{\mu}^{-1/2}N^2(1-N^4). \tag{68}$$

Figure 4 compares the analytic solution Eq.(68) with that of the numerical solution of Eq.(51). For the parameter of the calculation, $\phi(\eta)$ is given as $\exp(-2.33\eta^2)$. The existence of the localized eigenmode solution with the marginal stability condition (τ=0) is confirmed.

The growth rate of the mode is decreased by the further enhancement of the transport coefficient μ and χ as is shown from Eqs.(64) and (65). The stabilization occurs for the finite values of $\hat{\chi}$ and $\hat{\mu}$. By obtaining the minimum of RHS of Eq.(65), the upper bound of α for the stability is calculated. For the analytic estimate, we assume that $N^4 \ll 1$, and Eq.(65) is simplified as

$$f_1(N) \simeq (1/2+\alpha-s)[N^{-2}+\{2+3s^2/(1/2+\alpha-s)\}N^2]. \tag{69}$$

The function $f_1(N)$ takes the minimum value f(s) at $N=N_*$, where

$$f(s) = (1+2\alpha-2s)\sqrt{\{2+3s^2/(1/2+\alpha-s)\}} \tag{70}$$

and

$$N_*^{-2} = \{2+3s^2/(1/2+\alpha-s)\}^{1/2}. \qquad (71)$$

(The solution Eq.(71) satisfies the assumption that $N^4<<1$.) If we neglect α-s, for the simplicity, the minimum f(s) is estimated as $\sqrt{2+6s^2}$. In the limit s=0, f reduces to $\sqrt{2}$. (More exact value is given from Eq.(65). The minimum is given as $25\sqrt{5}/32$. The value of $\sqrt{2}$ is a good approximation for our interest.) We have the stability limit of α for the least stable mode as

$$\alpha^{3/2} = f(s)\sqrt{\hat{\mu}}\hat{\varkappa}^{3/2}\hat{\lambda}^{-1}, \qquad (72)$$

where f is given by Eq.(70). If $|\alpha-s|<<1$ holds,

$$f(s) \simeq \sqrt{2+6s^2}. \qquad (73)$$

When shear is strong and the mode is driven by the geodesic curvature, stability boundary is obtained, and f is given as (Yagi et al. 1993)

$$f(s) \sim 1.25s^2. \qquad (74)$$

3.4 Modes Not Localized at η=0

The potential $V(\eta)=\cos\eta+s\eta\sin\eta$ has many minima in addition to $\eta\simeq 0$. All modes are not localized at η=0, and the strong localized approximation may not always hold. We here discuss the mode which has maximum amplitude at $\eta=\eta_j$.

The minimum of the potential V is given at $\eta=\eta_{j*}$ which satisfies the condition

$$s\eta = (1-s)\tan\eta. \tag{75}$$

The solution is approximately given by $\eta_{j*}\simeq(2j+1/2)\pi$ $(j=1, 2, \cdots)$ for the case of $s\simeq 1$. Expanding the potential near $\eta=\eta_{j*}$, we have

$$V(\eta)=s\eta_{j*}\{1-(\eta-\eta_{j*})^2/2\}. \tag{76}$$

The marginal stability equation is approximated as

$$\frac{\partial^2}{\partial u^2}\Phi + \frac{\alpha\hat{\lambda}n^2q^2s\eta_{j*}}{\hat{\chi}}\{1-\frac{u^2}{2}\}\Phi - \hat{\mu}\hat{\lambda}n^6q^6F_*^3\Phi = 0 \tag{77}$$

where $u=\eta-\eta_{j*}$ and $F_*=F(\eta_{j*})$. The dispersion relation is given as

$$\sqrt{s\eta_{j*}\alpha} = \frac{\sqrt{2\hat{\chi}}}{\sqrt{\hat{\lambda}}4nq} + \sqrt{\frac{\hat{\chi}}{8\hat{\lambda}n^2q^2} + s^6\eta_{j*}^6\hat{\mu}\hat{\chi}n^4q^4} \tag{78}$$

The least stable mode satisfies

$$nq = \frac{1}{s\eta_{j*}}\left[\frac{5}{32\hat{\mu}\hat{\lambda}}\right]^{1/6} \tag{79}$$

For this mode number, the pressure gradient satisfies

$$\alpha = s\eta_{j*}\left[\frac{25}{32}\left(\frac{32}{5}\right)^{1/3}\frac{\hat{\varkappa}}{\hat{\lambda}}\left(\hat{\lambda}\hat{\mu}\right)^{1/3}\right] \tag{80}$$

Compared to Eq.(72), these modes (j=1, 2, ····) have higher stability boundary compared to the mode which is localized near η=0 for the parameter of s≃1.

4. Transport Coefficient and Fluctuations in Tokamaks

Based on the stability analysis, we derive the formula for the anomalous transport coefficient. When the mode amplitude and accordingly the associated transport coefficients are small, the mode is unstable (Eq.(61)). The mode continues to grow until Eq.(72) is satisfied. In the self-sustained turbulent state, the enhanced transport coefficients has the relation to the given pressure gradient α (Eq.(72)). This state is thermodynamically stable, namely, the excess growth of the mode and enhanced transport coefficients lead to the damping of the mode.

4.1 Formula of the Transport Coefficient

From Eq.(72), $\hat{\chi}$ is expressed in terms of the Prandtl numbers $\hat{\mu}/\hat{\chi}$ and $\hat{\lambda}/\hat{\chi}$. (Note that $\hat{\lambda}$ comes from the electron viscosity μ_e; Schmidt et al. 1971, Kaw et al. 1979.) We have

$$\hat{\chi} = f(s)^{-1}\alpha^{3/2}(\hat{\lambda}/\hat{\chi})\sqrt{\hat{\chi}/\hat{\mu}}. \qquad (81)$$

Use of the Prandtl numbers to notify the state is convenient, because the fluctuation amplitude less affects the ratio of transport coefficients, $\hat{\lambda}/\hat{\chi}$ and $\hat{\mu}/\hat{\chi}$, compared to the transport coefficients themselves, $\{\mu, \lambda, \chi\}$. To obtain the explicit expression for the transport coefficient, the Prandtl numbers are set to be constant. From Eqs.(43)-(45), we have the ion Prandtl

number as

$$\hat{\mu}/\hat{\chi} \simeq 1 \tag{82}$$

and the relations between the ion viscosity and the electron viscosity as

$$\mu \simeq \mu_e \tag{83-1}$$

for electrostatic perturbations. The electron Prandtl number, μ_e/χ, nearly equals to unity, or the relation

$$\hat{\lambda}/\hat{\chi} \simeq \delta^2/a^2 \tag{83-2}$$

holds. Substituting these relations Eqs.(82) and (83) into the expression of χ, Eq.(81), the formula of χ is reduced to

$$\hat{\chi} = f(s)^{-1}\alpha^{3/2}(\delta/a)^2, \tag{84-1}$$

or to an explicit form of

$$\chi = \frac{q^2}{f(s)}\left[\frac{R}{r}\frac{\partial\beta}{\partial\hat{r}}\right]^{3/2}\delta^2\frac{v_A}{R} \tag{84-2}$$

It is noted that the estimation of χ, by use of τ/k^2 for the most unstable mode, gives the same results as $\hat{\chi}\sim \alpha^{3/2}(\delta/a)^2$.

This result is compared to the Ohkawa formula (Ohkawa 1978)

$$\chi_{Ohkawa} = \delta^2 \frac{v_A}{qR} \{\frac{v_e}{v_A}\} \qquad (85)$$

which has shown that the typical scale length is the collisionless skin depth, δ, and the time scale of v_A/qR with finite pressure correction of $\sqrt{m_i\beta/m_e}$. By performing the renormalization of the nonlinear dynamics, we demonstrate his original idea, concerning on the scale length and the unit of the time. In addition, our theory is constructed to include the profile and geometrical factors of the plasma. The contribution from the pressure gradient and the magnetic shear are correctly incorporated in the formula Eq.(84).

The formula Eq.(84) quantifies the effect of the magnetic shear, which is favourable on the confinement. The contribution of the magnetic well, (which has also been considered to be favourable for the confinement,) does not appear in Eq.(84). It is a straightforward manipulation to include the effect of the well as a κ-term in the formula of the thermal conductivity. The correction of the form of $(1+C_1\kappa)$ appears in Eq.(84), where C_1 is a numerical coefficient of the order of unity, and the correction is of the order of the inverse aspect ratio, ε. The main features are unaltered. However, the existence of a small but finite magnetic well is essential to constrain the most unstable mode to be the ballooning mode. The case of the magnetic hill is treated later in §6. In such a case, the interchange mode can be unstable, leading to the anomalous transport coefficient which is

a strong increasing function of the magnetic hill.

4.2 Characteristics of the Thermal Conductivity

First, the dimensional dependence of χ is given

$$[\chi] \sim [T]^{1.5}/[a][B]^2, \qquad (86)$$

representing that the global thermal transport $[\chi]$ becomes larger when the average plasma temperature $[T]$ increases. The dimensional dependence is similar to that obtained from the quasilinear estimates of drift wave fluctuations and of ion-temperature-gradient modes (for a review, see Callen 1992).

Secondly, the formula Eq.(84-2) clarifies that the anomalous transport is driven by the *gradient* of β, not by the pressure itself. The essential feature of the anomalous transport, that the gradient generates the enhancement of χ, is predicted. As the pressure gradient increases, the heat flux increases nonlinearly. Figure 5 shows the dependence of the heat flux on ∇T for the fixed value of the density profile. When the temperature gradient is weak, χ is independent on ∇T. As the temperature gradient scale length becomes shorter than the density scale length, the heat flux nonlinearly increases with respect to ∇T.

Thirdly, the radial profile of χ is governed by the density and q profiles as well. The transport coefficient χ has the dependence on δ^2, and the collisionless skin depth δ is larger

near edge. (Note that the density is lower near edge). The q value is usually larger near edge. Our result of χ, Eq.(84), shows that χ increases towards the edge. This result agrees with the χ-profiles observed in the L-mode. Figure 6 illustrates the radial profile of the thermal transport coefficient predicted by our theory. Parameters are chosen from JFT-2M experiments (Ida et al. 1992) as B=1.2T, q(a)=1.2, T(0)=1keV, $n(0)=3\times10^{19}m^{-3}$, a=0.35m and R=1.3m. Profiles are chosen as $\beta(\hat{r})=\beta(0)(1-\hat{r}^2)$, $n_i(\hat{r})/n_i(0) = T(\hat{r})/T(0)$, $q(\hat{r}) = q(0)+\{q(a)-q(0)\}\hat{r}^2$. The conductivity χ takes the value in the range of 1 to 10 m^2/s. The radial shape, that χ is increasing towards the edge, is shown.

4.3 Typical Mode Structure

Characteristics of the self-sustained turbulence is evaluated from the nature of the most unstable mode.

The scale length is estimated from the mode number n. The normalized mode number $N=nq(\hat{\chi}\hat{\mu}/\alpha)^{1/4}$ for the most unstable mode, N_*, is given as of the order of unity.

When the shear is small but finite (i.e., the mode is driven by the normal curvature), an approximate value is given as $N_* \simeq f(s)^{-1/2}$. Therefore the mode number n is given as

$$nq = (\alpha/\hat{\chi}\hat{\mu})^{1/4} f(s)^{-1/2}. \qquad (87)$$

Employing the relation $\hat{\mu}=\hat{\chi}$, the typical perpendicular wave number of the most unstable mode satisfies

$$k_\perp \delta \simeq 1/\sqrt{\alpha}. \qquad (88)$$

It should be noticed that $k_\perp$ does not scale with the local gyroradius though the dimensional relation $k_\perp \propto [B]/[\sqrt{T}]$ holds. The collisionless skin depth, δ, is the more relevant length.

When the geodesic curvature drives the mode, the shear dependence of the mode number for the least stable mode is studied numerically (Yagi et al. 1993). The result shows that $N_* = 1/\sqrt{3}$, and the approximate relation

$$n \propto s^{-1} \qquad (89)$$

holds. This indicates that the longer wave length mode is expected to appear for the high shear case. For the typical parameters of $\mu=\chi$, $\lambda=\chi/1000$, $q=3$ and $\alpha=0.432$, n is close to 10.

The correlation time τ_c is estimated as $1/\hat{\gamma}$. From the expression of the growth rate, Eq.(61), and (87), and using Eq.(81), we have

$$\hat{\gamma} \sim \alpha^{1/2} f(s)^{-1/5} s^{-2/5}. \qquad (90\text{-}1)$$

An approximate form of τ_c is given as

$$\tau_c \simeq \sqrt{6s/\alpha}\,\tau_{Ap}. \qquad (90\text{-}2)$$

This expression also shows that the pressure gradient, not the

local pressure itself, is the key parameter to determine the correlation time. When the pressure gradient increases, the correlation time becomes shorter.

Mode amplitude can be estimated from Eq.(84). By the definition of μ, the order estimate

$$\mu \sim |k_{1\perp}\Phi_1/B|^2/\tau \tag{91}$$

holds. Writing $k_{1\perp}\Phi_1$ as $\tilde{E}$, this relation can be written as

$$\frac{\tilde{E}}{B} \simeq \frac{a}{qR}\sqrt{\hat{\mu}\hat{\tau}}\, v_A \tag{92}$$

Substituting the expressions of $\hat{\tau}$, $\hat{\mu}$ and $\hat{\chi}$, we have

$$\frac{\tilde{E}}{B} \simeq \frac{\delta}{qR}\alpha[s^{-1/5}f(s)^{-3/5}]\, v_A \tag{93}$$

The mode amplitude is larger for the higher pressure gradient (i.e., for the higher heating power). The shear dependence is favourable ($\tilde{E}/B \sim s^{-4/5}$). The normalized velocity $\tilde{E}/Bv_{Ti}$ is approximately rewritten as ($1/L_p = |\nabla p/p|$)

$$\frac{\tilde{E}}{Bv_{Ti}} \simeq \frac{\delta\sqrt{\alpha}}{\sqrt{RL_p}s^{4/5}} \tag{94}$$

where v_{Ti} is the ion thermal velocity, and the approximate relation $\beta=v_{Ti}^2/v_A^2$ is used. The turbulence velocity is much smaller than the thermal velocity. The fluctuation level, $\phi = \tilde{E}/k$, is estimated as

$$\frac{e\phi}{T} \simeq \sqrt{\frac{m_e}{m_i}}\,\frac{\delta}{L_p}\,\frac{q}{s^{4/5}}\,\sqrt{\alpha} \qquad (95)$$

where the relation $k_\perp\delta \sim 1/\sqrt{\alpha}$ is used. The normalized level of turbulence is shown to depend on the plasma profile and geometrical factor. The bigger the plasma is, the smaller the relative amplitude becomes.

5 Comparison with L-Mode Discharge of Tokamak

The form of χ is consistent with experimental results known for the L-mode. In the following, we compare the theoretical prediction to observations by choosing $n_i=n_e$ and $T_i=T_e$.

5.1 Local Thermal Conductivity

Two characteristic features of the local thermal conductivity in experiments are that (1) the value of χ is larger when the pressure gradient is larger, and that (2) the radial form of χ is increasing toward the edge. These are the commonly observed on the L-mode plasma. Figure 6 shows the theoretical prediction and also illustrates the range of the experimental observation for the JFT-2M tokamak plasma (Ida et al. 1992). The theoretical prediction (solid line) is slightly smaller than the experimental observation (shaded region) by the factor of 2 or so, but the radial shapes agree with each other.

The experiments to study the parameter dependence of χ have recently been performed. The dependences on the magnitude of the magnetic field and the strength of the magnetic shear are reported as

$$\chi \sim B_p^{-y} s^{-z} \qquad (96\text{-}1)$$

$$1<y<2 \text{ and } 0<z<1 \qquad (96\text{-}2)$$

from JET tokamak (Challis et al. 1992). The important role of the poloidal magnetic field, not the toroidal magnetic field, which is predicted in Eq.(84), is confirmed. The result Eq.(96) is consistent with Eq.(84). Analysis on the JT-60 experiment was reported in a form of

$$\chi \propto q^{3/2}\sqrt{\beta}\,\frac{\rho_i}{a}\,\frac{T}{eB} \tag{97}$$

(Takizuka 1992). This result is qualitatively consistent with the theoretical prediction.

The preliminary conclusion on the α-dependence of χ has been given on the JET experiment (Thomas 1987), which suggests the form

$$\chi \propto \alpha/\alpha_c \tag{98}$$

where α_c is the critical pressure gradient against the ideal MHD instability. The theoretical formula is written, apart from the slow shear dependence, as

$$\chi \propto (\alpha/\alpha_c)^{1.5}. \tag{99}$$

The qualitative agreement is found. In deriving Eq.(99), the approximate relation (Connor, et al. 1979) $\alpha_c \sim \sqrt{s}$ is used.

The gradual increase of the thermal conductivity with

respect to the increment of ∇T is reported (Alikaev et al. 1987). This fact is also reported from JET (Keilhacker et al. 1992). These observations are consistent with the theoretical prediction Eq.(84).

5.2 Scaling Study

The energy balance argument based on the point model,

$$\tau_E = a^2/\chi \qquad (100\text{-}1)$$

and

$$2\pi^2 a^2 R n_e T = \tau_E P, \qquad (100\text{-}2)$$

provides the scaling law. Using Eq.(84) and (100) and eliminating the averaged temperature T, we have

$$\tau_E = C\, a^{0.4} R^{1.2} I_p^{0.8} P^{-0.6} A^{0.2} f^{-0.4} n_e^{0.6} L_p^{0.6}, \qquad (101)$$

where C is a numerical coefficient, A is the ion mass number, and L_p is the gradient scale length of the pressure, $(nT)/|\nabla(nT)|$.

This result is consistent with the L-mode scaling law, including the dependences on a, R, I_p, P and also the favourable dependences on the ion mass A and magnetic shear f (Yushmanov et al. 1990, Zarnstorff, et al. 1991). Slight difference is seen in the density dependence in Eq.(101), which requires some

consideration. Since χ of Eq.(84) is dimensionally independent of the density, τ_E of Eq.(101) includes the density dependence (see, e.g., Lackner et al. 1990).

There are two possible reasons to explain the density dependence of τ_E in the L-mode plasmas. Firstly, the density dependence can be offset by the gradient scale length. In the L-mode plasmas, the high density plasma has more steeper edge density gradient; Tsuji found that $n_e(0)/\overline{n}_e$-1 is a decreasing function of $\overline{n}_e$ and $L_n\overline{n}_e$ is an weak function of the density (Tsuji 1992). (Since the density gradient profile is often steeper than the temperature near edge, L_p in Eq.(101) would be replaced by $L_n=|n_i/\nabla n_i|$.) The other reason is that the formula Eq.(101) is for the thermal component of the plasma energy. The usual L-mode scaling is often taken for the total energy which includes the energetic ions generated by the neutral beam injection. This energetic component is larger for the lower density plasma, and makes the density dependence of the total plasma energy less apparent. [For some dataset of JT-60, Takizuka reported the dependence as $\tau_E(\text{thermal}) \propto \overline{n}_e^{0.5}$ (Takizuka 1992).] These results suggest that the classification of the dataset by the profile is necessary.

5.3 Profile Resilience and ℓ_i dependence

The strong dependence of χ on the pressure gradient and on the magnetic shear can explain the experimental observations on the 'profile resilience' (Coppi 1980, Furth 1986) and the improvement

of the confinement time by the current peaking (Zarnstorff et al. 1991, Simonen et al. 1992, JT-60 Team 1992).

The temperature profile $T_e(r)$ is predicted from Eq.(84). To illustrate the effect of the plasma profile on χ (through the β', q and s dependences), we solve the energy transport equation,

$$q_{heat} = -\chi n \nabla T. \tag{102}$$

A simple form of the power absorption P_{abs} is chosen as

$$P_{abs}(x) = P_0 \exp\{-(x-x_{heat})^2/\Delta^2\} \tag{103}$$

where x is the radius measured along the pencil beam of NBI, and parameters x_{heat} and Δ characterize the location of the power absorption. For the simplicity, we assume $|\nabla n/n| << |\nabla T/T|$ and choose the q-profile

$$q(r) = q_0 + \{q(a)-q_0\}(r/a)^2 \tag{104}$$

The boundary condition is chosen as $T(a)=0$, and q_0 is set to satisfy the condition $q=1$ at $r/a=1/q(a)$.

Figure 7 shows the total plasma energy, i.e., the volume averaged plasma temperature $\langle T \rangle$ in this case, and the peaking parameter $T(\text{at } q=1)/\langle T \rangle$ as a function of the location of the peak heat absorption or the edge q-value. The total stored energy weakly depends on the location of the heat deposition, x_{heat}. The peaking parameter, $T(\text{at } q=1)/\langle T \rangle$, is also found to be weakly

dependent on the location of the peak of the power deposition. This explains the experimental observation on the weak dependence of T profile on the heating profile (See, e.g., Cordey et al. 1987).

The peaking parameter depends strongly on q(a). (See Fig.8.) The result is fitted as

$$T(q=1)/\langle T\rangle \sim q(a)^{0.6}. \qquad (105)$$

These results may explain the 'profile resilience'. (Experimental data was fitted to $T(0)/\langle T\rangle \sim q(a)^{2/3}$ in Waltz et al. (1986). Equation (105) is consistent with the data.) The strong dependence of the thermal conductivity on the temperature gradient resists against the change of the temperature gradient.

The dependences on shear and on the poloidal magnetic field cause the ℓ_i dependence of τ_E (ℓ_i: internal inductance). The solution of Eqs.(102)-(104) for the fixed value of q(a) are summarized in Fig.9. (In drawing Fig.9, the internal inductance is varied by changing q(0).) It is shown that, higher the internal inductance is, larger the energy confinement time becomes. This result is consistent with experimental observations (Zarnstorff et al. 1991, Simonen et al. 1992, JT-60 Team 1992),

$$\tau_E \propto \ell_i. \qquad (106)$$

The s- and q-dependences of the thermal transport coefficient is

confirmed at least qualitatively from the experimental observations.

5.4 Heat Pulse Propagation

The nature that the transport coefficient is a strong function of the gradient can also be tested by studying the pulsative response of the plasma. From the relation $\chi \propto \{\nabla(nT)/n\}^{1.5}$, the thermal diffusion coefficient deduced from the heat pulse propagation, χ_{HP}, is larger than that evaluated by the power balance χ.

The variation of the heat flux associated with the perturbation of the temperature is calculated from the formula of Eq.(84). We assume that the perturbation is limited to the temperature, and the density, current and velocity are assumed to be unchanged. Writing $T = T_0 + T_1$ and $q_{heat} = q_{heat,0} + q_{heat,1}$, we have

$$q_{heat,1} = -2.5n\chi_{PB}\nabla T_1 + 1.5n\chi_{PB}\left|\frac{T_0\nabla n_0}{\nabla(n_0T_0)}\right|\nabla T_1$$

$$+1.5n\chi_{PB}\left|\frac{\nabla n_0\nabla T_0}{\nabla(n_0T_0)}\right|T_1 \qquad (107)$$

where χ_{PB} is defined as

$$q_{heat,0} = -n\chi_{PB}\nabla T_0. \qquad (108)$$

If the density gradient is weak, i.e., the relation $|\nabla n/n| << |\nabla T/T|$ holds, we have the effective thermal diffusivity associated with the heat pulse,

$$-\chi_{HP} \equiv q_{heat,1}/(n_i \nabla T_1), \tag{109}$$

as

$$\chi_{HP}=2.5\chi. \tag{110}$$

If the equilibrium temperature profile is flatter, $|\nabla n/n| >> |\nabla T/T|$, then we have

$$\chi_{HP} = \chi. \tag{111}$$

For the case of comparable temperature and density gradients, $|\nabla n/n| \sim |\nabla T/T|$, the heat convection term (the last term in Eq.(107)) appears.

5.5 Characteristics of Fluctuations

The typical perpendicular wave number of the most unstable mode satisfies $k_\perp \delta \simeq 1/\sqrt{\alpha}$ as in Eq.(88). The dimensional relation $k_\perp \propto [B]/[\sqrt{T}]$ holds. Experimental observations have been performed (Mazzukato 1976, Surko and Slusher 1983, Surko 1987, Crowley and Mazzucato 1985). An experimental relation was given

$$\Delta k \propto B \tag{112}$$

by Surko (1987). The linear B dependence is consistent with Eq.(88).

The mode amplitude is predicted as Eq.(95). It is shown theoretically that the bigger the plasma is, the smaller the relative amplitude becomes. The dimensional dependence which is derived from Eq.(95) is

$$e\phi/T \propto [\sqrt{T}][a]^{-1}[B]^{-1}. \tag{113}$$

Experimental data was summarized in Liewer (1985) as, apart from dimensionless parameters,

$$\tilde{n}/n \sim 3\rho_i/L_n. \tag{114}$$

This result is consistent with the theoretical prediction, Eq.(95).

It is also shown in Eq.(95) that the mode amplitude becomes larger for the higher pressure gradient (i.e., for the higher heating power). The enhancement of the fluctuation level associated with the increased heating power was reported (For instance, TFR Group 1984).

The result Eq.(93) shows that the mode amplitude is large near plasma edge (δv_A dependence). The radial form of the fluctuation level shows the increase towards the edge (Durst et al. 1992).

These comparison shows that the experimental result on fluctuations are, at least qualitatively, consistent with our theoretical predictions.

6. Study for the System with Magnetic Hill

The theory can also be applied to the system with magnetic hill, such as torsatron/heliotron plasmas. In this case, the average magnetic hill allows a perturbation of interchange type (Rosenbluth and Longmire 1957).

6.1 Model

We use a model equation based on the reduced set of equations for stellarators (Strauss 1980). The cylindrical geometry is employed, and the case of zero equilibrium current is considered, to look for the analytical insight. The model equations consist of the Ohm's law, equation of motion and the energy balance equation. Replacing $\nabla(r\cos\theta)$ in Eq.(47) by the average hill term, we have

$$m_i n_i \left(\frac{\partial}{\partial t}\nabla_\perp^2\phi - \mu\nabla_\perp^4\phi\right) = B^2\nabla_{/\!/} J + B\Omega' \frac{\partial}{r\partial\theta}p, \tag{115}$$

$$\partial\psi/\partial t = -\nabla_{/\!/}\phi - J/\sigma + \lambda\nabla_\perp^2 J, \tag{116}$$

$$\partial p/\partial t = \frac{dp_0}{Bdr}\frac{\partial}{r\partial\theta}\phi + \chi\nabla_\perp^2 p, \tag{117}$$

where Ω' is the effective curvature of the vacuum field and is

defined as

$$\frac{d\Omega}{dr} = \frac{m}{R^2 \bar{\ell} r^2} \frac{d}{dr}(r^4 \iota) \tag{118}$$

where m is the toroidal pitch of the system, $\bar{\ell}$ is the multipolarity and ι is the rotational transform, $\iota = 1/q$. Since the mode is treated as the interchange mode (i.e., the variation in the envelope of the mode structure along the field line is neglected), the operator $\nabla_{//}$ is defined as

$$R\nabla_{//} = (\partial/\partial\zeta - \iota\partial/\partial\theta). \tag{119}$$

We solve the eigenvalue equation by the Fourier transformation. The normalization is the same as in the previous sections. The variable is changed from $x=\hat{r}-\hat{r}_1$ to k (r_1 being the mode rational surface) as

$$\Phi(x) = \exp[\hat{\tau}\hat{t} + im\theta - in\zeta] \int \Phi(k)\exp(ikx)dk \tag{120}$$

where m and n are poloidal and toroidal mode numbers, respectively. Eliminating J and p, we have the eigenvalue equation in the k space as

$$\frac{1}{L^2} \frac{\partial}{\partial k} \frac{1}{1/\hat{\sigma} + \hat{\lambda}k^2} \frac{\partial}{\partial k} \Phi + \frac{D}{\hat{\tau} + \hat{\chi}k^2} \Phi - (\hat{\tau}k^2 + \hat{\mu}k^4)\Phi = 0, \tag{121}$$

where $k^2 = k_\theta^2 + k^2$, $k_\theta = m/\hat{r}_1$,

$$1/L = k_\theta s, \tag{122-1}$$

$$D = D_0 k_\theta^2 \tag{122-2}$$

$$D_0 = -\frac{R^2}{2r^2}\frac{d\beta}{d\hat{r}}\frac{d\Omega}{d\hat{r}} \tag{122-3}$$

and D_0 denotes the driving by the pressure gradient. In the following k_θ denotes the normalized poloidal wave number, $m/\hat{r}$.

6.2 Current Diffusive Instability

Firstly, we confirm the large growth rate of the current diffusive mode by the WKB method. New coefficients G and υ as

$$G = 1/\hat{\sigma} + \hat{\lambda} k_\theta^2 \tag{123-1}$$

$$\upsilon = \hat{\lambda}/G \tag{123-2}$$

and new variable $\hat{k}$ as

$$d\hat{k}/dk = 1 + \upsilon k^2, \tag{124}$$

are introduced. The WKB solution of the most unstable mode satisfies the eigenvalue equation, i.e.,

$$\frac{\pi}{4} = \int_0^{\hat{k}_c} d\hat{k}\ Q, \tag{125}$$

and

$$Q = L\sqrt{\frac{G}{(1+\upsilon k^2)}\left[\frac{D}{(\hat{\tau}+\hat{\chi}k^2)} - (\hat{\gamma}k^2+\hat{\mu}k^4)\right]}, \tag{126-1}$$

$$Q(\hat{k}_c) = 0. \tag{126-2}$$

The asymptotic form of the mode growth rate is studied in the limit of large growth rate, i.e.,

$$\hat{\tau} > \hat{\chi}k^2,\ \hat{\mu}k^2. \tag{127}$$

In this limit, Eq.(125) reduces to

$$\frac{\pi}{4} = L\sqrt{G}\int_0^{\hat{k}_c} d\hat{k}\sqrt{\frac{1}{1+\upsilon k^2}\left[\frac{D}{\hat{\tau}} - \hat{\gamma}k^2\right]}. \tag{128}$$

The turning point $\hat{k}_c$ is given by the relation $k = \sqrt{D}/\hat{\tau}$. Taking the limit $\upsilon >> \hat{\tau}^2/D$, the dispersion relation is approximated as (Itoh et al. (1992c))

$$L\sqrt{\hat{\chi}}D^{3/2}\hat{\tau}^{-5/2} = 3\pi/4. \tag{129}$$

This relation yields the growth rate of the current-diffusivity driven mode as

$$\hat{\tau} = (4/3\pi)^{2/5} s^{-2/5} \hat{\lambda}^{1/5} k_\theta^{4/5} D_0^{3/5}. \qquad (130)$$

The growth rate of the mode is proportional to $\lambda^{1/5}$, as is the case of the ballooning mode in tokamaks,.

To obtain the most unstable mode structure, Eq. (121) is solved by Rayleigh-Ritz method. Writing Eq.(121) as $L\,u=0$, the functional $R[u]$ is defined as

$$R[u] = \int u L u dk / \int u^2 dk. \qquad (131)$$

Test function of

$$u=\exp(-\ell^2 k^2/2) \qquad (132)$$

is employed. Equations

$$R[u]=0 \qquad (133\text{-}1)$$

$$\partial R[u]/\partial \ell = 0 \qquad (133\text{-}2)$$

determine the growth rate τ and the typical structure of the mode, ℓ. The value ℓ denotes the radial extent of the mode. The Rayleigh quotient R is obtained as

$$R = -s^2\hat{\lambda}^{-1}\ell^2\{y^2-2y^3\exp(y^2)\mathrm{Erfc}(y)\} + 2D_0k_\theta^2\bar{\zeta}\exp(\bar{\zeta}^2)\mathrm{Erfc}(\bar{\zeta})$$

$$-\hat{\tau}k_\theta^2\{1+1/2y^2\} -\hat{\mu}k_\theta^4\{1+1/y^2+3/4y^4\} \qquad (134)$$

where $y=\ell^2k_\theta^2$, $\bar{\zeta}=\ell^2(\hat{\tau}/\hat{\chi}+k_\theta^2)$, and $\mathrm{Erfc}(y)=\int^{\gamma}\exp(-v^2)dv$. [Resistivity contribution is small if $1/\hat{\sigma} < \hat{\lambda}k_\theta^2$. This condition is satisfied, as shown a posteriori, and $1/\sigma$ is neglected.] In order to obtain the physics insight, we obtain the analytic expression, and assume that $\hat{\chi} \simeq \hat{\mu}$. (It is straightforward to study the general case of arbitrary ratio of μ/χ (Prandtl number), but this does not change the result qualitatively.)

In the large ℓk_θ limit, the asymptotic limit of the function Erfc is used. Taking the leading term in ℓk_θ (note $\hat{\chi} = \hat{\mu} = \hat{\tau}\ell^2$), the eigenvalue equation $R[u]=\partial R[u]/\partial\ell=0$ gives the growth rate and the radial extent ℓ of the fast interchange mode (Greene and Johnson 1961) as

$$\hat{\tau}=\sqrt{D_0}/(\ell k_\theta)^2 \qquad (135)$$

$$\ell^2=\sqrt{\hat{\lambda}(\hat{\tau}+2\hat{\mu}k_\theta^2)}/s. \qquad (136)$$

For the small ℓk_θ limit, the Taylor expansion of R is used. The first order term is written as

$$\hat{\tau} \simeq (\sqrt{8}/5)\ell k_\theta\sqrt{D_0}. \qquad (137)$$

From these results, the largest growth rate is given for the poloidal mode number satisfying

$$k_\theta \ell \sim 1. \tag{138}$$

For such mode, we have the estimate

$$\hat{\tau} \simeq \sqrt{D_0} \tag{139-1}$$

$$\ell^2 \simeq s^{-1}\sqrt{\hat{\lambda}\sqrt{D_0}}. \tag{139-2}$$

This result has been confirmed by Miller by numerical calculation. The maximum value of $\hat{\tau}$ was obtained as $0.25\sqrt{D_0}$ (Miller 1992).

6.3 Transport Coefficient

The stability boundary is calculated for the current diffusive interchange mode, and the transport coefficient is derived, as in the case of the ballooning mode.

Following the analysis of §3.3, the marginal stability condition (Eq.(121) with $\tau=0$) is simplified by neglecting the Φ' term as

$$\frac{\partial^2}{\partial k^2}\Phi + \frac{D_0\hat{\lambda}}{s^2\hat{\chi}}\Phi - \frac{\hat{\lambda}\hat{\mu}k_p^6}{s^2k_\theta^2}\Phi = 0, \tag{140}$$

where $k_p^2 = k_\theta^2 + k^2$. Introducing the normalization

$$b = k_\theta^2 (\hat{\mu}\hat{\lambda}/s^2)^{1/3} \tag{141-1}$$

$$z^2 = k^2 (\hat{\mu}\hat{\lambda}/s^2)^{1/3} \tag{141-2}$$

and the notation

$$H = \left[\frac{D_0 \hat{\lambda}}{s^2 \hat{\chi}}\right] \left[\frac{s^2}{\hat{\mu}\hat{\lambda}}\right]^{1/3} , \tag{141-3}$$

Eq.(140) is rewritten as

$$d^2\Phi/dz^2 + [(H-b^2) - G_1 z^2 - G_2 z^4 - G_3 z^6]\Phi = 0 \tag{142}$$

where $G_1 = 3b$, $G_2 = 3$, and $G_3 = 1/b$. Neglecting G_1 and G_2 as in Yagi et al. 1993, we have the stability boundary, by use of the WKB method, as

$$(H-b^2)^{2/3} b^{1/6} \int_0^1 \{1-x^6\}^{1/2} dx = \frac{\pi}{4} \tag{143}$$

H is a function of b as

$$H = b^2 + Cb^{-1/4} \tag{144-1}$$

where C is a constant defined by

$$C \equiv \left[\frac{4}{\pi}\int_0^1 \{1-x^6\}^{1/2}dx\right]^{-3/2}. \qquad (144\text{-}2)$$

The eigenvalue H has a minimum H_* of

$$H_* = (9/8^{8/9})C^{8/9} \qquad (145)$$

at

$$b_* = (C/8)^{4/9}. \qquad (146)$$

By combining the results of Eq.(141) and (145), we obtain the transport coefficient

$$\hat{\chi} = \frac{1}{H_*^{3/2}}\frac{D_0^{3/2}}{s^2}\frac{\hat{\lambda}}{\hat{\chi}}\left[\frac{\hat{\chi}}{\hat{\mu}}\right]^{1/2} \qquad (147)$$

The same argument, that the ratios μ_e/χ and μ/χ are order of unity, is applied as in the case of the ballooning mode in tokamaks. Equation (145) is rewritten as $H_*^{-3/2} \simeq 0.8$. Noting the normalization, and the explicit form of χ is finally obtained as,

$$\chi = F(\hat{r})\{d\beta/d\hat{r}\}^{3/2}\epsilon^2 v_A R^{-1} \qquad (148)$$

where $F(\hat{r})$ is the geometry-dependent numerical coefficient

$$F(\hat{\iota}) = \frac{0.8}{s^2}\left[\frac{m}{2}\frac{1}{\bar{l}}\frac{1}{r^4}\frac{d}{dr}(\iota r^4)\right]^{3/2}. \qquad (149)$$

The form of the thermal transport coefficient has the same β' dependence as that obtained for the tokamaks. The geometrical dependence is explicitly given in Eq.(148).

6.4 Comparison with Experiments

We discuss what is predicted from this model, comparing to the experimental results. Couple of similarity is found in the predictions on the torsatron/heliotron with those for tokamaks.

Firstly, the dimensional dependence of χ is

$$[\chi] \propto [T]^{1.5}/[R][B]^2 \qquad (150)$$

and is independent of the density, [n].

Secondly, the formula χ includes the radial dependence $(\beta'/n)^{3/2}$, not $T^{3/2}$, and predicts a large transport near edge. With this radial dependence and that of $F(\hat{\iota})$, χ is larger near the edge (Itoh et al. 1992a). The theoretical prediction of χ, that χ is larger for the high temperature or near the edge, is consistent with the result of experimental observations (Sano et al. 1990).

Third, the heat pulse propagation time is the same as in §4. For the case where $|\nabla T/T| >> |\nabla n/n|$ holds, χ_{HP} satisfies the

relation

$$\chi_{HP} = 2.5\ \chi_{eff}. \qquad (151)$$

The larger thermal conductivity for the heat pulse, than the equilibrium thermal conductivity, was observed in Heliotron E plasma (Zushi 1991).

There are differences from the case of tokamaks. Namely, these are due to the geometrical and configurational dependence.

The point model analysis gives the energy transport scaling law as

$$\tau_E = A^{0.2} B^{0.8} n^{0.6} a^2 R P^{-0.6} \langle F \rangle^{0.4} \qquad (152)$$

where $\langle F \rangle$ is the average of F near the boundary. (The reason to choose the edge value is discussed in Itoh and Itoh 1991.) The weak but positive dependence on the mass ratio is obtained. We find that the improvement of the confinement by the increase of the shear (s^{-2} term in F) is almost offset by the increment of the magnetic hill ($\{m(r^4\iota)'\}^{3/2} r^{-6}$ term in F). The coefficient $\langle F \rangle^{0.4}$ weakly depends on geometrical parameters. The energy confinement time depends mainly on the toroidal magnetic field, not on the poloidal magnetic filed. This result may explain the fact from the comparison study of experimental data in different devices, that τ_E seems to depend only weakly on the rotational transform or on the magnetic shear (Sudo et al. 1990). The predicted indices to B, n, a, R, and P, as a whole, are

consistent with the experimental scaling law (Sudo et al. 1990).

The nature of fluctuations are predicted by the theory. Since the mode is an interchange type, not a ballooning type, the features are different from those in tokamaks.

The ratio between the relative amplitude of density and potential fluctuations, $\tilde{n}/n$ and $e\phi/T$, is derived. The convective change dominates in $\tilde{n}$, and we have the relation

$$\tilde{n}/n=(\omega_*/\gamma)e\phi/T, \tag{153}$$

where ω_* is the drift frequency, $Tk_\theta/L_n eB$ (we assume that $T_e=T_i$). Using the condition $k_\theta \ell \simeq 1$ and the expressions for γ and ℓ, we have

$$\tilde{n}/n \simeq [3.1sD_0^{-1}\beta(a)R/L_n]\ e\phi/T. \tag{154}$$

From this relation we see that the density fluctuation is usually smaller than the potential fluctuation. For the case of Heliotron-E plasma, $D_0 \sim 60a\beta(0)/L_p$ and $s\sim 4$, that gives

$$\tilde{n}/n \sim [2(L_p/L_n)^2\beta(a)/\beta(0)]e\phi/T. \tag{155}$$

The value in bracket [ ] is order of 10^{-1}. Fluctuation measurements in high power heating experiments have shown that $\tilde{n}/n$ is smaller than $e\phi/T$ (Zushi, et al. 1988, Ritz et al. 1991), which confirms our model theory. This relation, Eq.(155), also suggests that $(\tilde{n}/n)/(e\phi/T)$ increases as the pressure profile

becomes broader. This prediction is also consistent with experimental results (Zushi et al 1988).

§7 Transport Coefficient in Stellarators

We here discuss the confinement of stellarator plasmas based on our theoretical model. The conventional stellarators such as the $\bar{l}=2$ stellarator are characterized by the magnetic well and the weak shear (Solov'ev and Shafranov 1970). Not an interchange mode but a ballooning mode must be analysed in this configuration (Cooper et al. 1989). We therefore apply the result of §3, taking the limit of $s \to 0$.

The thermal transport coefficient is obtained as

$$\chi = 0.6 q^2 (R\beta'/r)^{3/2} \delta^2 v_A / R. \tag{156}$$

The similarity is prominent with tokamaks rather than torsatron/Heliotron configurations.

We compare the prediction of the transport theory with observations. We choose the simplification $n_i = n_e$ and $T_i = T_e$, as in the case of tokamaks and torsatron/Heliotron.

(i) The dimensional dependence of χ is

$$[\chi] \sim [T]^{1.5}/[a][B]^2. \tag{157}$$

(ii) The *gradient* of β generates χ so that the density and q profiles govern the radial profile of χ. Equation (156) indicates that χ increases towards the edge for the usual plasma profiles in the L-mode. The increment of the thermal

conductivity near the edge was also confirmed in Wendelstein stellarators (Grieger et al. 1986).

(iii) The estimate, $\tau_E = a^2/\chi$ and $2\pi^2 a^2 R n_e T = \tau_E P$, provide the scaling law

$$\tau_E = C\, a^{2} R^{0.4} B^{0.8} \iota^{0.8} P^{-0.6} A^{0.2} \{n_e \ell_p\}^{0.6}, \qquad (158)$$

where C_s is a numerical coefficient. This result predicts the positive ι dependence of τ_E.

(iv) The $T_e(r)$ profile shows the difference from tokamaks. The peaking parameter, $T(0)/\langle T\rangle$, only weakly depends on the safety factor at edge, $q(a)$. This is because the safety factor q is almost uniform in stellarators and the change of the edge rotational transform does not cause the modification of the shape of $\chi(r)$ through q^2 and s. This is in contrast to the case of tokamaks. This explains the observations that the 'profile resilience' is not prominent in stellarators (Wagner 1992). The radial shape of χ can be different from that in tokamaks due to the same reason: The radial increment of χ in tokamaks is partly owing to the radial shape of $q(r)$. The flat $q(r)$ profile in stellarators leads to a flatter shape of $\chi(r)$ in stellarators, if profiles of density and pressure are common.

(v) The similar argument to those in previous sections applies to χ_{HP}. This value can be larger than that evaluated by the power balance χ.

(vi) The typical perpendicular wave number of the most unstable mode satisfies

$$k_{\perp}\delta \simeq 1/\sqrt{\alpha}. \qquad (159)$$

The correlation time τ_c is estimated as $1/\gamma \simeq \sqrt{1/\alpha}\tau_{Ap}$.

(vii) The estimate $\tilde{p}/p$ shows that the mode amplitude becomes large towards the edge and is larger for high heating power.

In our present theory, the toroidal mode is treated as a continuous variable. This implies that the rotational transform is not the low-order rational number (i.e., when ι is rational number and is written using the two integers as m_1/n_1, n_1 is not a small integer.) Therefore the theory may not be applicable to the case where ι is very close to the rational numbers such as 1/3, 1/2 and so on. The corrugations were found in the ι dependence of τ_E (See e.g. Grieger 1986). This is not included in the present theory. (The role of the magnetic island, for instance, is discussed in Wobig et al. 1987).

§8 Summary and Discussion

In this article we developed the theory for the self-sustained turbulence and the associated anomalous transport in toroidal plasmas. The geometrical effects such as the toroidicity, magnetic shear and magnetic well are incorporated. The mode is driven by the pressure gradient. The E×B nonlinearity is taken into account. Nonlinear interactions are renormalized in a form of diffusion effects on the microscopic mode. By use of the mean field approximation, the set of transport coefficients $\{\mu_k, \lambda_k, \chi_k\}$ are represented by a single set of scalar diffusion coefficients $\{\mu, \lambda, \chi\}$. The stability analysis of the microscopic ballooning mode in toroidal plasmas are done under the influence of the anomalous transport coefficients χ, λ and μ. It is found that this mode becomes unstable when the transport is small and finite, by the effect of self-induced current diffusivity, λ. The modes can be stabilized by the enhanced anomalous transport, i.e., the thermal transport, χ, and the ion viscosity, μ. The marginal stability condition is obtained, and the condition for the stationary state of the self-sustained turbulence is obtained. The transport coefficients are rewritten in terms of the Prandtl numbers. The Prandtl numbers are little affected by the fluctuation amplitude, so that they are assumed to be constant. The formula of the anomalous transport coefficient is thus derived. The important role of the collisionless skin depth, which was first pointed out in Ohkawa's model, is theoretically demonstrated: The consistent calculation

for stability gives more explicit dependence on β' and on the geometrical factor.

The formula of the anomalous transport which is caused by the pressure-gradient-driven instabilities can be summarized in a form as

$$\chi = F(\hat{r})\left[\frac{d\beta}{d\hat{r}}\right]^{3/2} \delta^2 \frac{v_A}{R} \tag{160}$$

where the geometrical factor F is given as

$$F(\hat{r}) = \begin{cases} q^2(R/r)^{1.5} f(s)^{-1} & \text{(tokamak)} \\ 0.6q^2(R/r)^{1.5} & \text{(Stellarator)} \\ F(\hat{r}) & \text{(torsatron/Heliotron)} \end{cases} \tag{161}$$

Approximate form of f(s) is given in Eqs.(70) and (74), and that of F is given in Eq.(149). The result clarifies the role of the pressure gradient as the origin of the anomalous transport in toroidal plasmas. Simultaneously, the effects of the magnetic shear and the magnetic well, both of which have been known as favourable for improving the stability of the toroidal plasmas, are clarified. The magnetic well has clearly improved the plasma confinement, as was demonstrated in literatures (see e.g. Ohkawa and Kerst 1961 and Yoshikawa 1973). The result in this article clearly shows the positive effect of the average magnetic well on

the anomalous transport.

The fluctuation level of the self-sustained turbulence is also given. For the ballooning mode turbulence in tokamaks, the formula

$$e\phi/T \simeq \sqrt{\alpha m_e/m_i}\ \delta q/(L_p s^{4/5}) \qquad (182)$$

is obtained. This result suggests the importance of the toroidal curvature and the pressure gradient for the driving source of instabilities in tokamaks. The geometrical factor, such as the safety factor, is included, confirming that the connection length is the key parameter for the stabilization of the ballooning mode. It is also noted that the level $e\phi/T$ depends, on the magnitude of the main magnetic field and plasma temperature through α. The plasma size has an important factor; the bigger the plasma, the lower the relative fluctuation level. The density is also influential; the level decreases if the density is increased. The typical wavenumber is also given. The collisionless skin depth, δ, is shown to be a relevant length to characterize the modenumber. The result $k\delta \propto 1/\sqrt{\alpha}$ shows that the typical mode number increases in proportion to B when the pressure and other parameters are kept constant. The characteristics of the fluctuations from our model theory are also consistent with those in experimental observations.

The results on χ are compared with experimental observations. Major part of the observations on L-mode in tokamak plasmas can be explained by this model, simultaneously.

In particular, this model explains not only the enhancement of the thermal conductivity due to the increase of temperature, but also the radial profile of χ, namely the larger value of χ towards the edge. The point model estimate of the energy confinement time, τ_E, is done. The empirical dependence of τ_E on the plasma current, ion mass number, plasma size and weak dependence on the toroidal magnetic field seems to be consistent with theoretical prediction. The dependences of χ on the pressure gradient and q(r) can explain so-called 'profile resilience' (Coppi 1980, Furth 1986). The recent observation, that the energy confinement time is improved by the increase of the internal inductance (Zarnstorff et al. 1991, Simonen et al. 1992, JT-60 Team 1992), is explained in the framework of this theory.

The theory also explains the various features, (which are common to tokamaks,) observed in experiments on stellarators (helical devices). Namely, the power degradation of τ_E, the increment of the thermal conductivity by the pressure gradient and the radial profile of the thermal conductivity, especially, are explained by this unified theory. The different features from tokamak plasmas have also been explained. For instance, the torsatron/Heliotron experiments have shown that τ_E depends on the main magnetic field, not on the poloidal magnetic field. High shear and high rotational transform not necessarily improve the energy confinement time. This observation is explained by this theory. The most unstable mode in these plasmas is the interchange mode, so that the poloidal magnetic field plays

little role. It is found that the increment of the shear, by the increase of the toroidal pitch number of the device, is offset by the increment of the magnetic hill. The hill has an unfavourable effects on confinement. It is also noticed that, among helical systems, the anomalous transport in the conventional stellarators and that in the torsatron/ Heliotron devices are different in many aspects. The confinement time in the conventional stellarator can depend on the rotational transform. It must be misleading if the regression analysis on the confinement time is performed on the mixed data from the conventional stellarator and torsatron/Heliotron devices.

Compared to the previous theories, this model provides a better understanding on the L-mode plasma. Only few theories have been successful in simultaneous explanation of the large χ value near the edge and the power degradation: one was the Ohkawa model (Ohkawa 1978) and the other is the critical-temperature gradient model (Rebut et al. 1987). The relation of this model with the Ohkawa model was explained. The expression of χ from the critical temperature gradient model is given as an inductive formula, and the theoretical derivation was not given.

In this article, the resistivity is neglected. The analysis is done for the resistive plasma to have the instability boundary

$$\alpha = \hat{\chi}\hat{\sigma}/2. \qquad (163)$$

The resistive modes (Carreras and Diamond 1989) give higher stability limit of α than the current diffusive modes if

$$\hat{\alpha}\hat{\chi}^{1/3} > (\hat{\chi}/\hat{\lambda})^{2/3} \qquad (164)$$

holds. Equation (164) is usually satisfied supporting the simplification in this analysis. The thermal conductivity of Eq.(163) is rewritten as $\chi = (4q^2R/L_p)\rho_e{}^2\nu_{ei}$, where ρ_e is the electron gyroradius and ν_{ei} is the electron-ion collision frequency. The Pseudo-classical diffusion coefficient (Yoshikawa 1970) is derived in the framework of this self-sustained turbulence. The takeover from Pseudo-classical confinement to the neo-Bohm (L-mode) confinement will be reported in a separate article.

The role of resistivity is important when the background fluctuation amplitude is small. In the limit of the zero amplitude of turbulence, the transport coefficient is given by the classical values. In such a case, the mode in unstable. The instability continues until the turbulence level grows and the marginal stability condition becomes to be satisfied. This is in contrast to the case of the drift wave turbulence discussed in Hirshman and Molvig (1979), where a fairly large threshold amplitude was required to excite the nonlinear instability.

The present theory gives the (approximate) formula

$$\chi \propto (\alpha/\alpha_c)^{1.5} \qquad (165)$$

where α_c is the critical stability limit of the ideal MHD instability. This result provides a picture that the efforts to look for the configuration with high MHD-beta limit may also allow the better energy confinement. The role of the current profile is analyzed in this article and confirmed this

conjecture. The effect of the plasma shaping must be studied to get the final conclusion. It is also worthwhile to investigate the case of the second stability (Coppi et al. 1979). Part of the analysis was performed in Yagi et al. 1993.

The other aspect to improve the confinement is the influence of the radial electric field (Itoh et al. 1989, Itoh and Itoh 1990, Shaing et al. 1989, Bigrali et al. 1988, Hassam 1991, Sugama and Wakatani 1991). The impact of the radial electric field on the self-sustained turbulence has been performed as an extension of the present theory. The result confirmed the previous theories that the electric field anisotropy reduces the transport. The details of the analysis will be reported in a forthcoming paper. It has also been pointed out that the off-diagonal elements in the transport matrix can lead important effects in the L-mode plasma (Itoh 1990, 1992, Ida et al 1992). In particular, the physics of the pinch phenomena requires the analysis on the off-diagonal elements. The off-diagonal term is also calculated in the framework of this theory. Application of this theory to the pinch phenomena will be discussed in future.

We assume the isotropy of the background turbulence, i.e., $\langle\langle|\partial\phi/\partial r|\rangle\rangle \simeq \langle\langle|\partial\phi/r\partial\theta|\rangle\rangle$. The generalization to the case of the anisotropic fluctuation $\langle\langle|\partial\phi/\partial r|\rangle\rangle \neq \langle\langle|\partial\phi/r\partial\theta|\rangle\rangle$ is possible. The Appendix B describes the generalization. It is concluded, *a posteriori*, that the anisotropy of the background turbulence does not change the conclusion of this article. Also necessary is the improvement of the evaluation of the Prandtl numbers μ_e/χ and μ/χ. A better estimate would be possible if the

values of $k_\perp$ and $k_{//}$, evaluated for the most unstable modes, are to be substituted in the expressions of $\{\mu, \lambda, \chi\}$.

Nonlinear stationary solution is obtained in this letter by taking the ansatz for χ, i.e., the transport coefficients affecting the microscopic mode is equated to that for the global quantity. Recently, Connor has succeeded to reproduce our results by use of the scale invariance technique, supporting our model (Connor 1993). It is also pointed out that the other form of the Ohm's law gives the higher thermal conductivity. In giving an alternate derivation of the Ohkawa's formula, the extension of the Ohm's law was discussed in (Kadomtsev and Pogutse 1985, Horton et al. 1987). The resistive term J/σ is replaced by the electron pressure term $\nabla p/en_e$. By this correction, the increment of the thermal conductivity was pointed out (Connor 1993). Even in this case, however, the fundamental feature of the anomalous transport, that

$$\hat{\chi} \propto f(s)^{-1}\alpha^{3/2}(\hat{\lambda}/\hat{\chi})(\hat{\chi}/\hat{\mu})^{1/2} \qquad (166)$$

is found unaltered.

This correction in Ohm's law is considered to be one of the finite gyroradius correction. The result of the typical wave number, $k\hat{\delta} \sim 1/2\sqrt{\alpha}$, suggests that k can be of the order of the ion gyroradius, when the pressure increases. The finite gyroradius effect on ions, contrary to that on electrons, can reduce the transport coefficient. The role of magnetic perturbation was also discussed (Lichtenberg et al. 1992, Connor

1993). The extension of this theory to such cases requires future analysis.

The precise numerical factor cannot be obtained from the present analysis. Though the fundamental structure of $\hat{\chi}$ is unaltered, the coefficients can be enhanced by the change of the electron parallel conductivity and by the magnetic perturbations. The detailed explanation of the absolute value requires future study. Nonlinear simulation would give this coefficient and can examine the validity of the ansatz. Other simplifications such as the neglect of the spatial inhomogeneity of the background turbulence must be examined in detail. The important role of the advection of fluctuation in the transition between L- and H-modes was theoretically predicted (Itoh and Itoh 1988). It has been pointed out (Yoshizawa 1984) that the incoherent convection of the background turbulence affects the level of turbulence in the stationary state. The method of two-scale direct renormalization approach can be applied to this problem, and may clarify the importance of the incoherent convection on this problem. It is also necessary to investigate the effects such as the kinetic corrections, parallel flow or perpendicular compressibility. These researches are open for future study.

Acknowledgements

Authors would like to acknowledge useful discussions with and comments by Drs. J. W. Connor and T. Ohkawa. They thank Dr. R. L. Miller for allowing them to quote his unpublished work. They also thank discussions with Drs. M. N. Rosenbluth, T. Takizuka, S. Tsuji, S. Yoshikawa, H. Niedermayer, H. Zushi, H. Sanuki, K. Ichiguchi and members of D-III D experimental group, JFT-2M group and Heliotron-E group. This work is partly supported by the Grant-in-Aid for Scientific Research of Ministry of Education Japan and by the collaboration program between universities and JAERI on fusion.

Appendix A Transport Matrix

Explicit form of the transport matrix, which is given by the ExB nonlinearity of the back-ground turbulence, is presented in this appendix.

The nonlinear terms (23)-(25) can be expressed in the matrix form. As is shown in Eqs.(13)-(15), the driven terms $\{U_2, J_2, p_2\}$ are given in the form of the combination of $\{N_1, N_2, N_3\}$. Substituting Eqs.(13)-(15) in Eqs.(23)-(25), we write

$$\begin{pmatrix} N_U \\ N_J \\ N_p \end{pmatrix} = \frac{1}{B^2}\Sigma \begin{pmatrix} H_{11} & H_{11} & H_{13} \\ H_{21} & H_{22} & H_{23} \\ H_{31} & H_{32} & H_{33} \end{pmatrix} \begin{pmatrix} [\Phi_{-1}, [\Phi_1, \tilde{U}]] \\ [\Phi_{-1}, [\Phi_1, \tilde{J}]] \\ [\Phi_{-1}, [\Phi_1, \tilde{p}]] \end{pmatrix} \qquad (A1)$$

where summation is taken over k_1. (The notation k_1 denotes the back-ground turbulence.) Using the expressions for $\{U_2, J_2, p_2\}$, the matrix elements H_{ij} are given as

$$H_{11} = \frac{k_{2\perp}^2}{K_2} \qquad (A2)$$

$$H_{12} = \frac{ik_{2/\!/}gk_{2\perp}^2}{K_2 \tau_{j2}} \qquad (A3)$$

$$H_{13} = \frac{A_2 k_{2\perp}^2}{K_2 \tau_{p2}} \qquad (A4)$$

$$\hat{H}_{21} = \mu_0 \delta^2 \frac{ik_{2\parallel}\xi}{K_2 \tau_{j2}} \tag{A5}$$

$$\hat{H}_{22} = \mu_0 \delta^2 \frac{1}{K_2} \frac{\tau_{u2}}{\tau_{j2}} \left[k_{2\perp}^2 + \frac{iA_2 k_{2\theta} \nabla p_0}{\tau_{u2} \tau_{p2} B} \right] \tag{A6}$$

$$\hat{H}_{23} = \mu_0 \delta^2 \frac{ik_{2\parallel}\xi A_2}{K_2 \tau_{j2} \tau_{p2}} \tag{A7}$$

$$H_{31} = \frac{-ik_{2\theta} \nabla p_0}{K_2 \tau_{p2} B} \tag{A8}$$

$$H_{32} = - \frac{k_{2\theta} \nabla p_0 g k_{2\parallel}}{K_2 \tau_{j2} \tau_{p2} B} \tag{A9}$$

and

$$H_{33} = \frac{1}{K_2} \frac{\tau_{u2}}{\tau_{p2}} \left[k_{2\perp}^2 + \frac{g\xi k_{2\parallel}^2}{\tau_{u2} \tau_{j2}} \right] \tag{A10}$$

The suffix 2 denotes the mode k_2 which is given as $k_2 = k_1 + k$, and the symbol $A_2 p_2$ indicates Ap(for k_2). (The notation k is for the test wave.) Eqs.(A2) to (A10) represent the explicit form of $\{H_{ij}\}$ in Eqs.(26) and (32) in the main text.

The transport matrix for the background plasma profile is also obtained by taking the limit of $k \to 0$. The conventional quasilinear treatment is used to obtain the diffusion operator

caused by the background perturbations. We write in the matrix form as

$$\frac{\partial}{\partial t}U - \frac{B^2}{m_i n_i}\nabla_{/\!/}J - \frac{B}{m_i n_i}\nabla p \times \nabla\left(\frac{2r\cos\theta}{R}\right)\cdot\hat{\zeta} =$$

$$D_{11}\nabla_\perp^2 U + D_{12}\nabla_\perp^2 J + D_{13}\nabla_\perp^2 p \qquad \text{(A11)}$$

$$-E - v\times B + \frac{1}{\sigma}J = \delta^2\mu_0\{D_{21}\nabla_\perp^2 U + D_{22}\nabla_\perp^2 J + D_{23}\nabla_\perp^2 p\} \qquad \text{(A12)}$$

$$\frac{\partial}{\partial t}p + \frac{1}{B}[\phi, p] = D_{31}\nabla_\perp^2 U + D_{32}\nabla_\perp^2 J + D_{33}\nabla_\perp^2 p \qquad \text{(A13)}$$

and

$$U = \nabla_\perp^2\phi. \qquad \text{(A14)}$$

The matrix elements $\{D_{ij}\}$ is given by taking the limit $k\to 0$ into the expressions $\{H_{ij}\}$ as

$$\begin{pmatrix} D_{11} & D_{12} & D_{13} \\ D_{21} & D_{22} & D_{23} \\ D_{31} & D_{32} & D_{33} \end{pmatrix} = \sum_{k_l} \frac{|k_{l\perp}\phi_l|^2}{2B^2} \begin{pmatrix} H_{11} & H_{11} & H_{13} \\ H_{21} & H_{22} & H_{23} \\ H_{31} & H_{32} & H_{33} \end{pmatrix}_{k\to 0} \qquad \text{(A15)}$$

The matrix elements $H_{ij}(k\to 0)$ in (A15) are explicitly given as

$$H_{11} = \frac{k_{1\perp}^2}{K_1} \tag{A16}$$

$$H_{12} = \frac{ik_{1/\!/}gk_{1\perp}^2}{K_1 \tau_{j1}} \tag{A17}$$

$$H_{13} = \frac{A_1 k_{1\perp}^2}{K_1 \tau_{p1}} \tag{A18}$$

$$H_{21} = \frac{ik_{1/\!/}\xi}{K_1 \tau_{j1}} \tag{A19}$$

$$H_{22} = \frac{1}{K_1} \frac{\tau_{u1}}{\tau_{j1}} \left\{ k_{1\perp}^2 + \frac{iA_1 k_{1\theta} \nabla p_0}{\tau_{u1} \tau_{p1} B} \right\} \tag{A20}$$

$$H_{23} = \frac{ik_{1/\!/}\xi A_1}{K_1 \tau_{j1} \tau_{p1}} \tag{A21}$$

$$H_{31} = \frac{-ik_{1\theta} \nabla p_0}{K_1 \tau_{p1} B} \tag{A22}$$

$$H_{32} = -\frac{k_{1\theta} \nabla p_0 g k_{1/\!/}}{K_1 \tau_{j1} \tau_{p1} B} \tag{A23}$$

and

$$H_{33} = \frac{1}{K_1} \frac{\tau_{u1}}{\tau_{p1}} \left(k_{1\perp}{}^2 + \frac{g\xi k_{1//}{}^2}{\tau_{u1}\tau_{j1}} \right) \tag{A24}$$

The symbol $A_1 p_1$ denotes Ap(for k_1). We write diagonal terms D_{11}, $\delta^2 \mu_0 D_{22}$ and D_{33} by μ, λ and $\varkappa$, respectively.

Appendix B Effect of Anisotropy of Turbulence

A set of renormalized equations are derived in §2 with an assumption of the isotropic turbulence,

$$|\partial\phi_1/\partial x|^2 \simeq |\partial\phi_1/\partial y|^2 \simeq |k_{1\perp}{}^2\phi_1|^2/2. \tag{B1}$$

The generalization to the case of anisotropic turbulence, $|\partial\phi_1/\partial x|^2 \neq |\partial\phi_1/\partial y|^2$ is possible. (The x- and y-directions are taken in the radial and poloidal directions, respectively.) We introduce the parameter W which denotes the anisotropy of the turbulence as

$$W \equiv \frac{\langle\langle |\partial\phi_1/\partial y|^2 \rangle\rangle}{\langle\langle |\partial\phi_1/\partial x|^2 \rangle\rangle} \tag{B2}$$

The bracket $\langle\langle\rangle\rangle$ indicates the average. We determine the anisotropy parameter W along the spirit of the mean field approximation. Namely, the ratio of the radial derivative of the test wave to the poloidal derivative equals to those of the background waves, $1/\sqrt{W}$.

By use of W, the nonlinear terms are rewritten as

$$[\phi_{-1}, [\phi_1, \tilde{Y}]] = \left|\frac{\partial\phi_1}{\partial x}\right|^2 \left(\frac{\partial^2}{\partial y^2} + W\frac{\partial^2}{\partial x^2}\right)\tilde{Y} \tag{B3}$$

and Eq.(30) is rewritten in the form of

$$\begin{pmatrix} N_U \\ N_J \\ N_p \end{pmatrix} = \Sigma \frac{|k_{1r}\Phi_1|^2}{2B^2} \begin{pmatrix} H_{11} & H_{11} & H_{13} \\ H_{21} & H_{22} & H_{23} \\ H_{31} & H_{32} & H_{33} \end{pmatrix} \Delta_a \begin{pmatrix} \tilde{U} \\ \tilde{J} \\ \tilde{p} \end{pmatrix} \qquad (B4)$$

where the operator Δ_a is defined as

$$\Delta_a \equiv \frac{\partial^2}{\partial y^2} + W\frac{\partial^2}{\partial x^2} \qquad (B5)$$

We only keep the diagonal terms in the matrix $\{H_{ij}\}$ in the following. The set of model equations are rewritten as

$$n_i m_i \{\partial(\nabla_\perp^2\Phi)/\partial t - \mu\Delta_a\nabla_\perp^2\Phi\} = B^2\nabla_{//}J + B\nabla p\times\nabla(2r\cos\theta/R)\cdot\hat{\zeta} \qquad (B6)$$

$$E+v\times B = \frac{1}{\sigma}J - \lambda\Delta_a J \qquad (B7)$$

and

$$\frac{\partial}{\partial t}p + \frac{1}{B}[\Phi, p_0] = \chi\Delta_a p. \qquad (B8)$$

The coefficients $\{\mu, \lambda, \chi\}$ are given as

$$\mu = \Sigma \frac{|k_{1r}\Phi_1|^2}{B^2} \frac{k_{1\perp}^2}{K_1} \qquad (B9)$$

$$\lambda = \delta^2 \mu_0 \mu_e \tag{B10-1}$$

$$\mu_e = \Sigma \frac{|k_{1r}\Phi_1|^2}{B^2} \frac{1}{K_1} \frac{\tau_{u1}}{\tau_{j1}} \left(k_{1\perp}^2 + \frac{iA_1 k_{1\theta} \nabla p_0}{\tau_{u1}\tau_{p1} B} \right) \tag{B10-2}$$

and

$$\chi = \Sigma \frac{|k_{1r}\Phi_1|^2}{B^2} \frac{1}{K_1} \frac{\tau_{u1}}{\tau_{p1}} \left(k_{1\perp}^2 + \frac{g\xi k_{1/\!/}^2}{\tau_{u1}\tau_{j1}} \right) \tag{B11}$$

where

$$K_1 = \tau_{u1} k_{1\perp}^2 + g\xi \frac{k_{1/\!/}^2}{\tau_{j1}} + \frac{iA_1 k_{1\theta} \nabla p_0}{\tau_{p1} B} \tag{B12}$$

$\tau_{u1}=\tau(1)+\mu k_{1\perp}^2$, $\tau_{j1}=\tau(1)+\mu_e k_{1\perp}^2$, $\tau_{p1}=\tau(1)+\chi k_{1\perp}^2$, and $\partial Y_1/\partial t = \tau(1) Y_1$.

The ballooning formalism is also employed. Following the same procedure, we have

$$\frac{d}{d\eta} \frac{F}{\hat{\tau}+\Xi F+\Lambda F F_a} \frac{d\phi}{d\eta} + \frac{\alpha[\kappa+\cos\eta+(s\eta-\alpha\sin\eta)\sin\eta]\phi}{\hat{\tau}+XF_a}$$

$$- (\hat{\tau}+MF_a)F\phi = 0 \tag{B13}$$

Comparing Eq.(B13) to Eq.(51) in the main text, a new geometrical

parameter F_a appears, which is defined as

$$F_a=1+W(s\eta-\alpha\sin\eta)^2, \tag{B14}$$

The operator $\nabla_\perp^2$ is transformed as $-n^2q^2F$.

Equation (B13) contains the parameter W, which is determined by the selfconsistent relation

$$\langle k_\theta{}^2\rangle/\langle k_r{}^2\rangle = W \tag{B15}$$

where the average $\langle\cdots\rangle$ is defined as

$$\langle X\rangle \equiv \frac{\int X\phi^2 dxdy}{\int \phi^2 dxdy} \tag{B16}$$

The ballooning transformation gives

$$\frac{\langle k_r{}^2\rangle}{\langle k_\theta{}^2\rangle} = \frac{\int s^2\eta^2\phi(\eta)^2 d\eta}{\int \phi(\eta)^2 d\eta} \tag{B17}$$

The stability boundary is derived. Setting $\hat{\tau}=0$ in Eq.(B13), we have the eigenvalue equation, which determines the relation between $\hat{\chi}$, $\hat{\lambda}$ and $\hat{\mu}$. As is in §3, we study the case that the ballooning mode is destabilized by the normal curvature, not by the geodesic curvature, i.e., $1/2+\alpha>s$. For the strongly localized mode, $s^2\eta^2<1$ and $\eta^2<1$, this eigenvalue equation is approximated by the Weber type equation, and Eq.(63) is modified

as

$$d^2\phi/d\eta^2 + (\alpha\hat{\lambda}n^2q^2/\hat{\chi})\{1-(1/2+\alpha-s)\eta^2\}$$

$$- \hat{\mu}\hat{\chi}n^6q^6\{1+(1+2W)s^2\eta^2\} = 0 \qquad \text{(B18)}$$

The marginal stability condition is given as

$$H = f_1(N) \qquad \text{(B19)}$$

where

$$H \equiv \alpha^{3/2}\hat{\lambda}\hat{\chi}^{-3/2}\hat{\mu}^{-1/2} \qquad \text{(B20-1)}$$

and

$$f_1(N) \equiv N^{-2}(1-N^4)^{-2}\{(1/2+\alpha-s)+(1+2W)s^2N^4\} \qquad \text{(B20-2)}$$

where N is the normalized mode number $N=nq(\hat{\chi}\hat{\mu}/\alpha)^{1/4}$ as in §3. The eigenmode structure is obtained by the gaussian form

$$\phi(\eta) = \exp\{-(\eta/\eta_0)^2\} \qquad \text{(B21)}$$

where

$$\eta_0^{-2} = H N^2(1-N^4)/2 \qquad \text{(B22)}$$

The integration Eq.(B17) is performed by using the form of $\phi(\eta)$ to have

$$\langle s^2\eta^2\rangle = \frac{s^2}{2H\,N^2(1-N^4)} \tag{B23}$$

The self-consistency relation Eqs.(B15) and B(17) lead to

$$s^2W = 2H\,N^2(1-N^4) \tag{B24}$$

Substituting Eq.(B24) into Eq.(B20), and neglecting higher order terms of N^4, we have

$$H = \left[\frac{1}{2}\right]\left[(1+2\alpha-2s)N^{-2}+\{6(1+2\alpha-2s)+2s^2\}N^2\right] \tag{B25}$$

The minimum of the right hand side of Eq.(B25) is given as $\sqrt{(1+2\alpha-2s)\{6(1+2\alpha-2s)+2s^2\}}$. When the $(\alpha-s)$ term is small and neglected, it reduces to $\sqrt{6+2s^2}$. The stability boundary for the least stable mode is given as

$$\alpha^{3/2}\hat{\lambda}\hat{\chi}^{-3/2}\hat{\mu}^{-1/2} = \sqrt{6+2s^2}. \tag{B26}$$

At this condition, the parameter W is given as

$$W = \frac{5+2s^2}{s^2(3+s^2)} \tag{B27}$$

The typical mode number of the least stable mode is given as

$$k_\theta \delta \simeq 1/\sqrt{\alpha}, \tag{B28}$$

which is the same result compared to that for the isotropic turbulence. The anisotropy parameter W becomes small and the radial correlation length becomes shorter when the shear becomes stronger.

Comparing Eqs.(84) and (B26), we see that the assumption of the isotropic turbulence in the main text gives a sufficiently good approximation. The anisotropy of the spectrum gives rise to a small difference in the marginal stability condition. The role of the plasma pressure gradient is not altered. The formula of χ is affected on the s-dependence, and the shear dependence is slightly weaker in Eq.(B26). Other dependences are not altered.

References

Alikaev V V, Bagdasarov A A, Berezovskij E L, Berlizov A B, Bobrovskij G A, Borshchegovskij A A, Vasin N L, Vertiporokh A N I, et al (1987): in *Plasma Physics and Controlled Nuclear Fusion Research 1986* (IAEA, Vienna, 1987) Vol.1, p111.

Bigrali H, Diamond P H, Terry P W (1989): Phys. Fluids **B2** 1.

Burrell K H , Gentle K W, Luhmann N C Jr, Marmar E S, Murakami M, Schoenberg K F, Tang W M, Zarnstorff M C, (1988): Nucl. Fusion **28** 3.

Callen J D (1992): Phys. Fluids **B4** 2142.

Carreras B A, Diamond P H (1989): Phys. Fluids **B1** 1011.

Challis C D, Christiansen J P, Cordey J G, Gormezano C, Gowers C W, Kramer G J, O'Rourke J J, et al. (1992): Nucl. Fusion **32** 2217.

Connor J W , and J B Taylor (1977): Nucl. Fusion **17** 1047.

Connor J W , Hastie R J , and J B Taylor (1979): Proc. R. Soc. London, **A365** 1.

Connor J W (1993): to be published in Plasma Physics and Controlled Fusion.

Cordey J G, Bartlett D V, Bhatnagar V, Bickerton R J, Bures M, Callen D J, Campbell D J, Challis C D, et al. (1987): in *Plasma Physics and Controlled Nuclear Fusion Research 1986* (IAEA, Vienna, 1987) Vol.1, p.99.

Cooper W A, Hirshman S P, and Lee D K (1989): Nucl. Fusion **29** 455.

Coppi B, Ferreira A, Mark J W-K, Ramos J J (1979): Plasma Physics Controlled Fusion 5 1.

Coppi B (1980): Comments on Plasma Physics and Controlled Fusion 5 261.

Crowley T and Mazzucato E (1985): Nucl. Fusion 25 507.

Dupree T H (1966): Phys. Fluids 9 1773.

Dupree T H (1972): Phys. Fluids 15 334.

Durst R D, Fonck R J, Cosby G, Evensen H, Paul S F: (1992): Rev. Sci. Instrum. 63 4907.

Furth H P (1986): Plasma Physics and Controlled Fusion 29 1305.

Goldston R J (1984): Plasma Phys. Control. Fusion 26 87.

Gouldon C, Marty D, Maschke E K, Dumon J P (1968): *Plasma Physics and Controlled Nuclear Fusion Research* (IAEA, Vienna, 1968) Vol.1, p847.

Greene J, Johnson J L (1961): Phys. Fluids 4 875.

Grieger G, W VII-A Team, NI-Team ECRH Group, Pellet Injection Group (1986): Plasma Phys. Controlled Fusion 28 43.

Hassam A B (1991): Comments on Plasma Physics Controlled Fusion 14 275.

Hirshman S P, and Molvig K (1979): Phys. Rev. Lett. 42 648.

Horton C W (1984): in *Basic Plasma Physics II* (*Handbook of Plasma Physics*, ed. by A. A. Galeev and R. N. Sudan, Vol.2, North-Holland, Amsterdam, 1984) p.411.

Horton C W, Choi D-I, Yushmanov P N, Parail V V (1987): Plasma Phys. Cont. Fusion 29 901.

Houlberg W A, Ross D W, Bateman G, Cowley S C, Efthimion P C, Pfeiffer W W, Porter G D, et al. (1990): Phys. Fluids B2

2913.

Ida K, Itoh K, Itoh S-I, Hidekuma S, JIPPT-IIU group, CHS Group (1991): in *Plasma Physics and Controlled Nuclear Fusion Research 1990* (IAEA, Vienna, 1991) Vol.2, p577.

Ida K, Itoh S-I, Itoh K, Miura Y and JFT-2M group (1992): Phys. Rev. Lett. **68** 182.

Itoh K and Itoh S-I (1991): Comments Plasma Phys. Cont. Fusion **14** 1.

Itoh K, Itoh S-I, Fukuyama A (1992a): Phys. Rev. Lett. **69** 1050.

Itoh K, Itoh S-I, Fukuyama A, Yagi M, Azumi M (1992b): in Proc. 14th Int. Conf. Plasma Phys. Cont. Nuclear Fusion Research, (IAEA, Wurzburg) paper H-2-2.

Itoh K, Ichiguchi K, Itoh S-I (1992c): Phys. Fluids **B4** 2929.

Itoh, K., Itoh S-I, Fukuyama A, Yagi M, Azumi M (1993): Plasma Physics and Controlled Fusion **35** in press.

Itoh S-I and Itoh K (1988): Phys. Rev. Lett. **60** 2276.

Itoh S-I, Itoh K, Ohkawa T, Ueda N (1989): in *Plasma Physics and Controlled Nuclear Fusion Research 1988* (Proc. 12th Int. Conf. Niece, 1988) Vol.2, p.23, IAEA, Vienna.

Itoh S-I (1990): J. Phys. Soc. Jpn. **59** 3431.

Itoh S-I and Itoh K (1990): J. Phys. Soc. Jpn. **59** 3815.

Itoh S-I (1992): Phys. Fluids **B4** 796.

Kadomtsev B B (1965): in Plasma Turbulence (Academic Press, New York).

Kadomtsev B B and Pogutse O P (1985): in *Plasma Physics and Controlled Nuclear Fusion Research 1984* (Proc. 10th Int.

Conf. London, 1984) Vol.2, p.69, IAEA, Vienna.

Kaw P J, Valeo E J, Rutherford P H (1979): Phys. Rev. Lett. **43** 1398.

Keilhacker M and JET Team (1992): presented in 14th Int. Conf. Plasma Physics and Controlled Nuclear Fusion, Wurzburg, (1992, IAEA), paper A-1-1.

JT-60 Team (1992): presented in 14th Int. Conf. Plasma Physics and Controlled Nuclear Fusion, Wurzburg, (1992, IAEA), paper A-1-3.

Lackner K, Gottardi N(1990): Nucl. Fusion **30** 767.

Lichtenberg A J, Itoh K, Itoh S-I, Fukuyama A (1992): Nucl. Fusion **31** 495.

Liewer P (1985): Nucl. Fusion **25** 543.

Mazzucato E (1976): Phys Rev. Lett. **36** 792.

Miller R L (1992): (private communications)

Mohri A (1970a): J. Phys. Soc. Jpn. **28** 1549.

Mohri A and Azumi M (1970b): J. Phys. Soc. Jpn. **29** 1580.

Ohkawa T and Kerst D W (1961): Phys. Rev. Lett. **7** 41.

Ohkawa T (1978): Phys. Letters **67A** 35.

Rebut P H, Lallia P P, Watkins M L (1989): in *Plasma Physics and Controlled Nuclear Fusion Research 1988* (Proc. 12th Int. Conf. Niece, 1988) Vol.2, p.191, IAEA, Vienna.

Ritz C P, Rhodes T L, Lin H, Rowan W L, Tsui H, Meier M, Bengston R D, Wootton A J, et al. (1991): *Plasma Physics and Controlled Nuclear Fusion Research 1990* (Proc. 13th Int. Conf. Washington, 1990) Vol.2, IAEA, Vienna p589.

Rosenbluth M N and Longmire C L (1957): Ann. Phys. **1** 120.

Ross D W, Bravenec R V, Ritz Ch P, Sloan M L, Thompson J R, Wootton A J, Schoch P M, et al. (1991): Phys. Fluids **B3** 2251.

Sano F, Takeiri Y, Hanatani K, Zushi H, Sato M, Sudo S, Mutoh T Kondo K, et al. (1990): Nucl. Fusion **30** 81.

Shaing K C, Lee G S, Carreras B A, Houlberg W A, Crume E C Jr (1989): in *Plasma Physics and Controlled Nuclear Fusion Research 1988* (Proc. 12th Int. Conf. Niece, 1988) Vol.2, p.13, IAEA, Vienna.

Simonen T C and D-III D Team (1992): in 14th Int. Conf. Plasma Physics and Controlled Nuclear Fusion, Wurzburg, (1992, IAEA), paper A-1-2.

Scott B D (1990): Phys. Rev. Lett. **65** 3289.

Schmidt J and Yoshikawa S (1971): Phys. Rev. Lett. **26** 753.

Solov'ev L S and Shafranov V D (1970): in *Reviews of Plasma Physics* (ed. M. A. Leontovich) Vol.5, p.1 (Consultants Bureau, New York, 1970).

Strauss H (1977): Phys. Fluids **20** 1354.

Strauss H (1980): Plasma Phys. **22** 733.

Sudo S, Takeiri Y, Zushi H, Sano F, Itoh K, Kondo K, Iiyoshi A (1990): Nucl. Fusion 11 **30**.

Surko C and Slusher R E (1983): Science 221 817.

Surko C (1987): Comments Plasma Phys. Controlled Fusion 10 265.

Sugama H and Wakatani M (1991): Phys. Fluids **B3** 1110.

Takizuka T (1992): in *Controlled Fusion and Plasma Heating* (Proc. 19th Eur. Conf. Innsbruck, Austria, 1992) Vol.16C, European Physical Society, (1992) Part 1, p51.

TFR Group (1984): Plasma Phys. Controlled Fusion **26** 1045.

Thomas P R (1987): 'A comparison between additional heating data forms with model scale invariance', JET report JET-P(87)17.

Tsuji S (1992): Fusion Engineering and Design **15** 311.

Uo K (1971): Plasma Physics **13** 243.

Wagner F (1992): invited talk in 19th Eur. Conf.Controlled Fusion and Plasma Heating, (Innsbruck, 1992).

Waltz R et al. (1986): Nucl. Fusion **26** 1729.

Wakatani M, Watanabe K, Sugama H, Hasegawa A (1992): Phys. Fluids **B4** 1754.

Wobig H, Maassberg H, Renner H, W VII-A Team, ECH Group, NI Group (1987): in *Plasma Physics and Controlled Nuclear Fusion Research 1986* (Proc. 11th Int. Conf. Kyoto, 1986) Vol.2, p.369, IAEA, Vienna.

Wootton A, Carreras B A, Matsumoto H, McGuire K, Peebles W A, Ritz Ch P, Terry P W, Zweben S J (1990): Phys. Fluids **B2** 2879.

Yagi M (1989): PhD Thesis, Kyoto University.

Yagi M, Itoh K, Itoh S-I, Fukuyama A, Azumi M (1993): 'Analysis of current diffusive ballooning mode', submitted to Physics Fluids.

Yoshikawa S (1970): Phys. Rev. Lett. **25** 353.

Yoshikawa S (1973): Nucl. Fusion **13** 433.

Yoshizawa A (1984): Phys. Fluids **27** 1377.

Yushmanov P, Takizuka T, Riedel K S, Kardaun O J W F, Cordey J G, Kaye S M, Post D E (1990): Nucl. Fusion **30** 1999.

Zarnstorff M C, Barnes C W, Efthimion P C, Hammet G W,

Horton W, Hulse R A Mansfield D K, et al. (1991): in *Plasma Physics and Controlled Nuclear Fusion Research 1990* (IAEA, Vienna, 1991) Vol.1, p109.

Zushi H, Mizuuchi T, Motojima O, Wakatani M, Sano F, Sato M, Iiyoshi A, Uo K (1988): Nucl. Fusion **28** 433.

Zushi H (1991): private communications.

Figure Captions

Fig.1 Geometry of the analysis.

Fig.2 (a) Growth rate of the current-diffusive ballooning mode as a function of β for various values of $\hat{\lambda}$. Dashed line shows the ideal MHD limit. (b) Growth rate as a function of $\hat{\lambda}$ for $\beta=0.8\%$. Parameters are: $s=0.4$, $\hat{\chi}/\hat{\lambda}=1000$, $\hat{\mu}=\hat{\chi}$, $q=3$, $r/L_p=0.6$, $\varepsilon=1/8$, $n=80$, and $1/\hat{\sigma}=0$.

Fig.3 Marginal stability condition as a function of the mode number n. Solid line indicates the analytic formula (65). Dashed line is obtained by the numerical calculation. Parameters are $s=0.4$, $\hat{\chi}=1.7\times10^{-5}$, $\hat{\chi}/\hat{\lambda}=1000$, $\hat{\mu}=\hat{\chi}$, $q=3$, $r/L_p=0.6$, $\varepsilon=1/8$, and $1/\hat{\sigma}=0$.

Fig.4 Eigenmode profile of the marginally stable mode. Solid line is the result of the numerical calculation and the dashed line is the analytical estimation. Parameters are: $s=0.4$, $\hat{\chi}=10^{-5}$, $\hat{\chi}/\hat{\lambda}=1000$, $\hat{\mu}=\hat{\chi}$, $q=3$, $r/L_p=0.6$, $\varepsilon=1/8$, $1/\hat{\sigma}=0$, and $n=78$.

Fig.5 Heat flux q_r is shown as a function of the temperature gradient. The density gradient is fixed. At the location denoted by the symbol *, the temperature gradient scale length $|T/\nabla T|$ is equal to that of the density $|n/\nabla n|$.

Fig.6 Radial profile of the thermal transport coefficient. Example of the parameters are chosen from JFT-2M tokamak plasma (Ida et al. 1992). Parameters are: B=1.2T, R=1.3m, a=.35m, $n(0)=3\times10^{19}m^{-3}$, T(0)=1keV, q(a)=3.2 and q(0)=1.0. The profiles are chosen $\beta(r/a)=\beta(0)\{1-(r/a)^2\}$ and $n(r)/n(0)=T(r)/T(0)$. The shaded area indicates the range of the experimental observation quoted from Fig.2 of Ida et al. 1992.

Fig.7 Dependence of the energy confinement time (a) and the peakedness of the temperature profile (b) on the location of the power deposition. The peaking parameter of the power deposition Δ is chosen as $\Delta/a=0.3$. x_{heat} indicates the position of the peak of the power deposition. Parameters are chosen q(a)=3 and $r_1/a=1/q(a)$ (r_1 is the location of the q=1 surface). Density profile is assumed to be flat and the boundary condition of T(a)=0 is used.

Fig.8 Dependence of the peakedness of the temperature profile on q(a). The peaking parameter of the power deposition Δ is chosen as $\Delta/a=0.3$, and peak position of the power deposition is given as $x_{heat}/a=0.5$. The location of the q=1 surface is given by $r_1/a=1/q(a)$. Density profile is assumed to be flat and the boundary condition of T(a)=0 is used.

Fig.9 Dependence of the energy confinement time on the

internal inductance ℓ_i. f(s) is modelled as f=1.7 (s<0.6) and $\sqrt{6}$s (s>0.6) for the simplicity. The internal inductance is varied by changing the central q value with the form $q(r)=q(0)+\{q(a)-q(0)\}(r/a)^2$ and q(a) is chosen as in Fig.8. The density profile is assumed to be constant, and T(a) =0.

Fig. 1

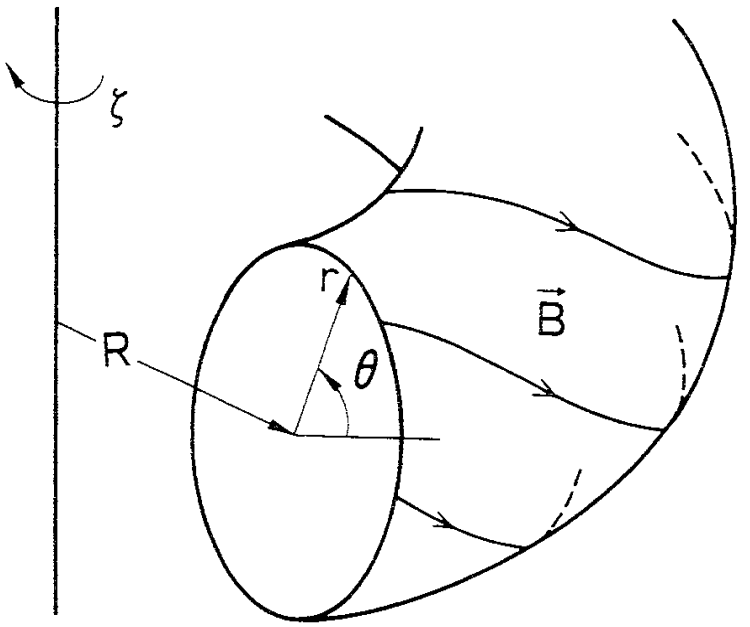

Fig. 2

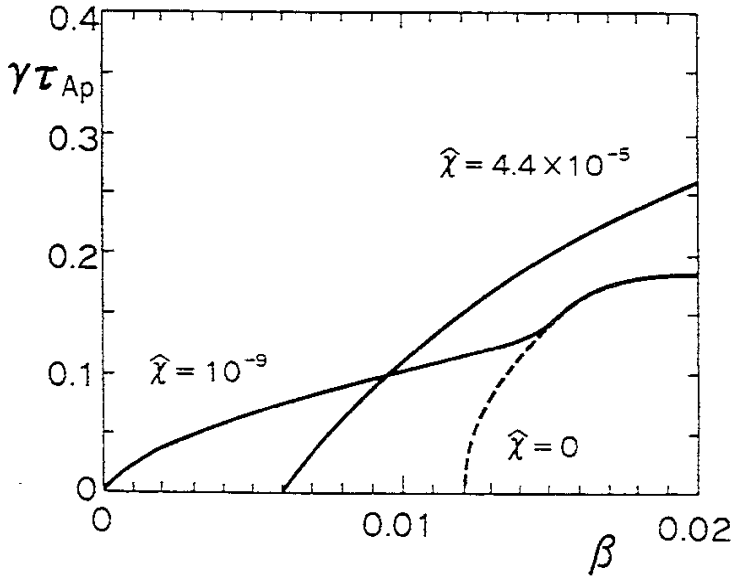
0.4
$\gamma\tau_{Ap}$
0.3
0.2
0.1
0
$\hat{\chi} = 4.4\times10^{-5}$
$\hat{\chi} = 10^{-9}$
$\hat{\chi} = 0$
0
0.01
0.02
β

(a)

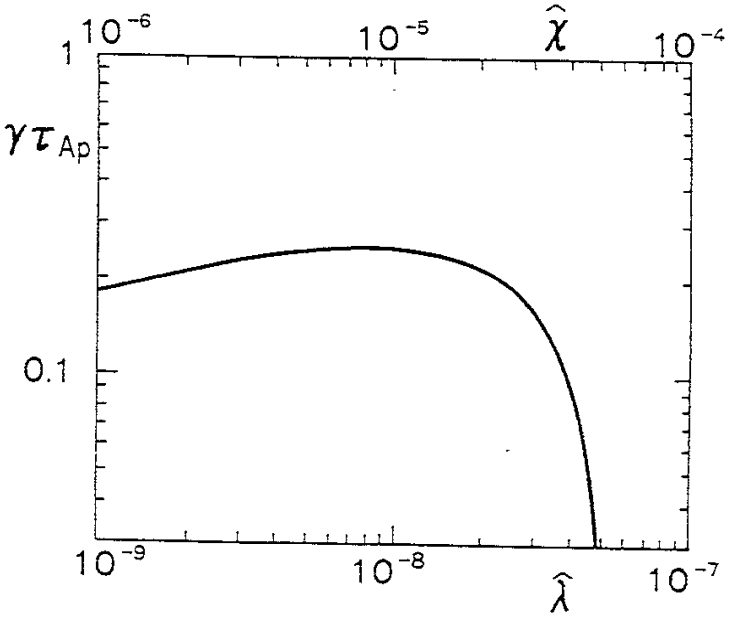
10^{-6}
10^{-5}
$\hat{\chi}$
10^{-4}
1
$\gamma\tau_{Ap}$
0.1
10^{-9}
10^{-8}
$\hat{\lambda}$
10^{-7}

(b)

Fig. 3

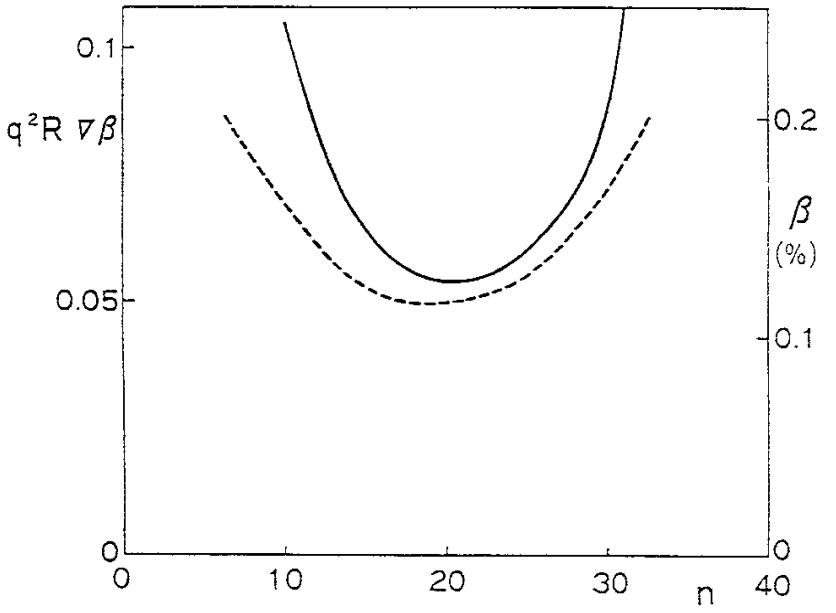

Fig. 4

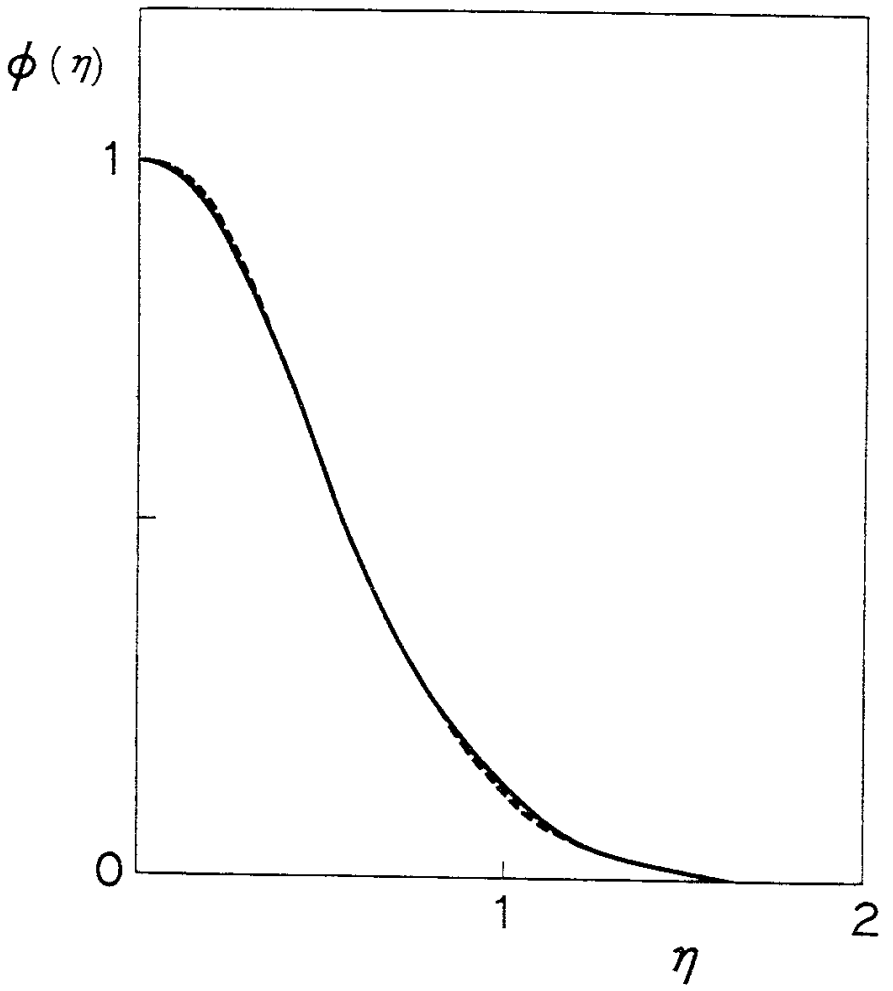

Fig. 5

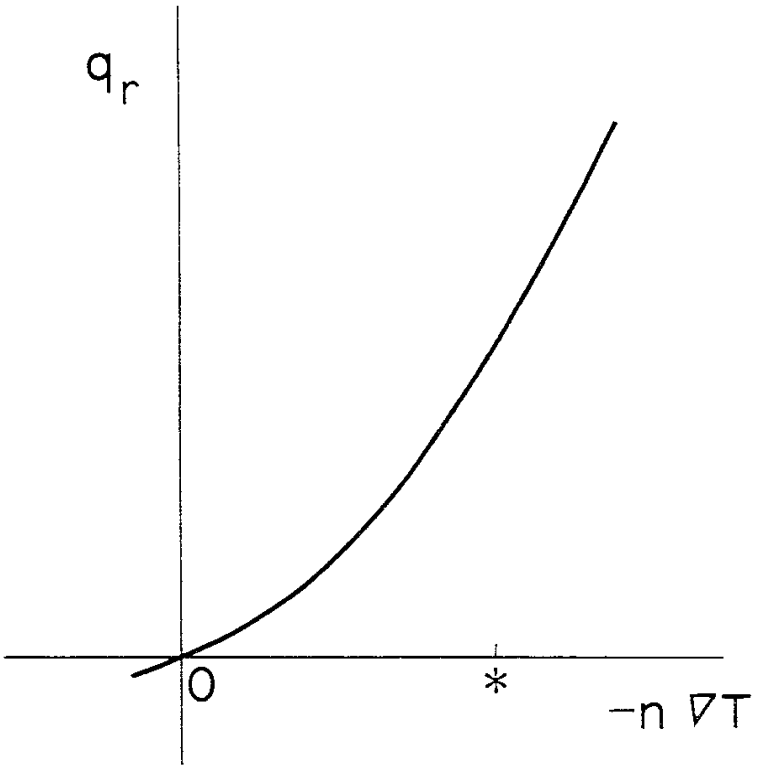

Fig. 6

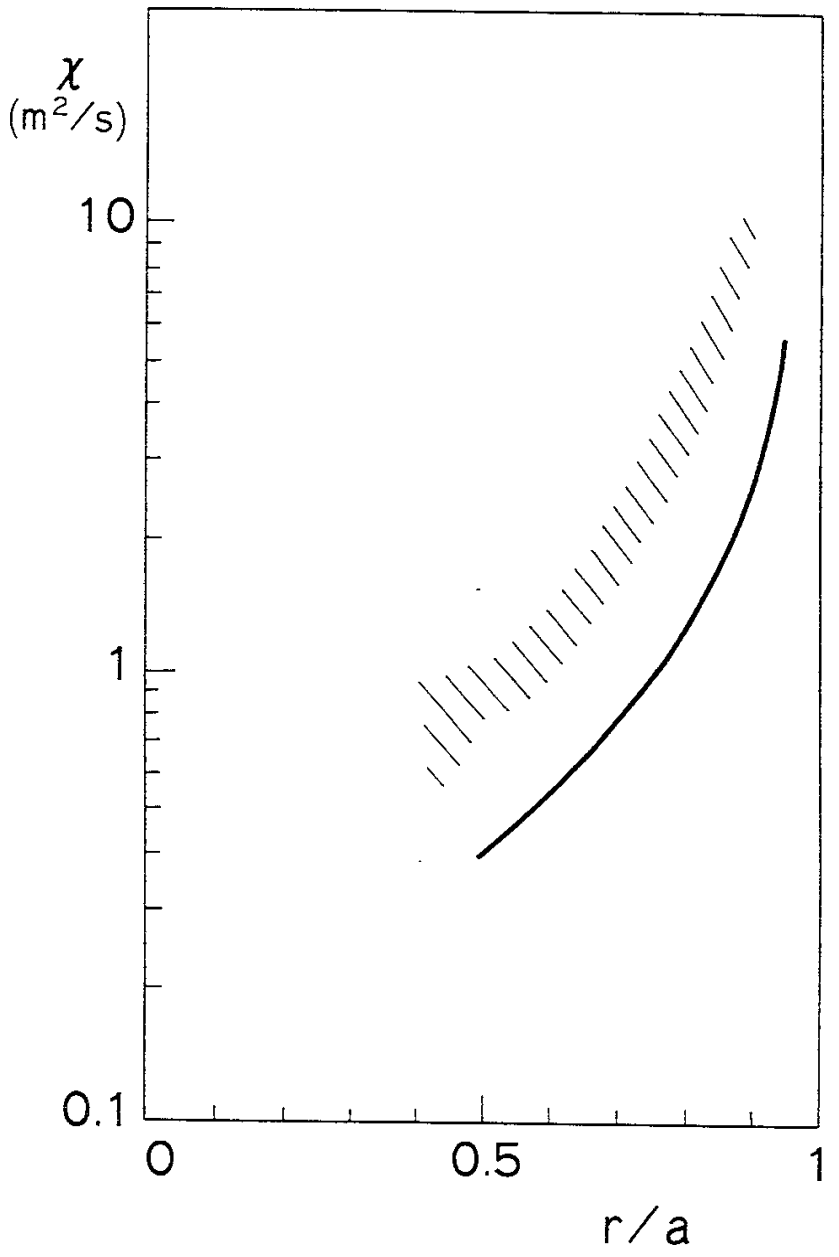

Fig.7

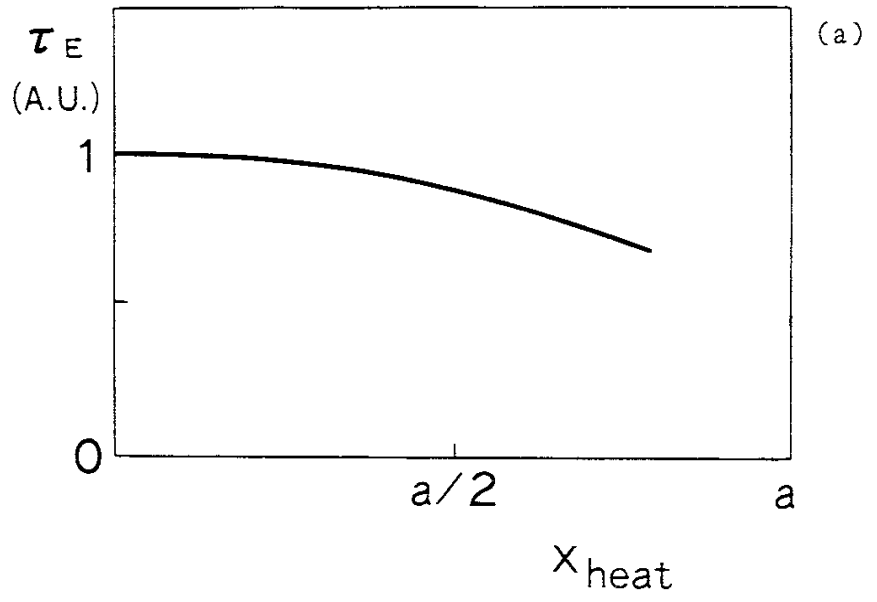
τ_E
(A.U.)
1
0
a/2
a
x_{heat}
(a)

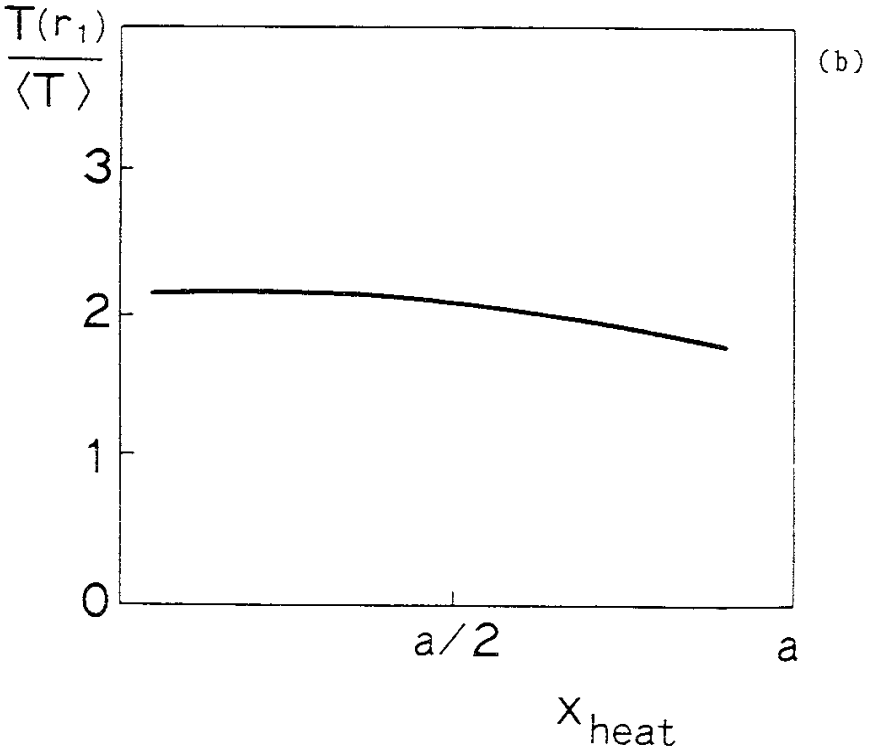
$\frac{T(r_1)}{\langle T \rangle}$
3
2
1
0
a/2
a
x_{heat}
(b)

Fig. 8

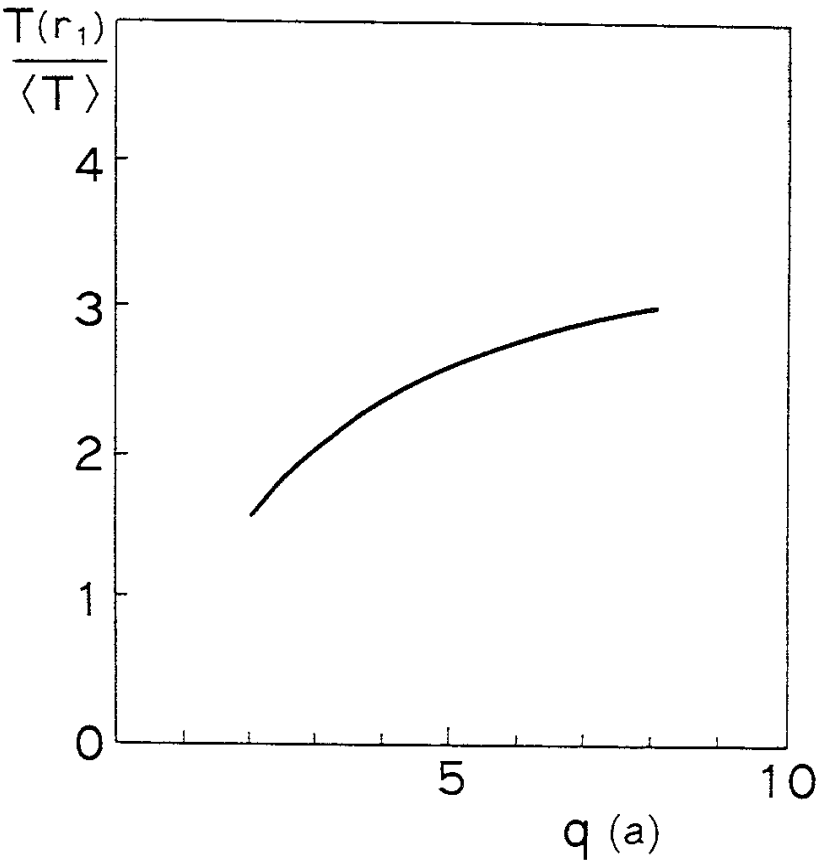

Fig. 9

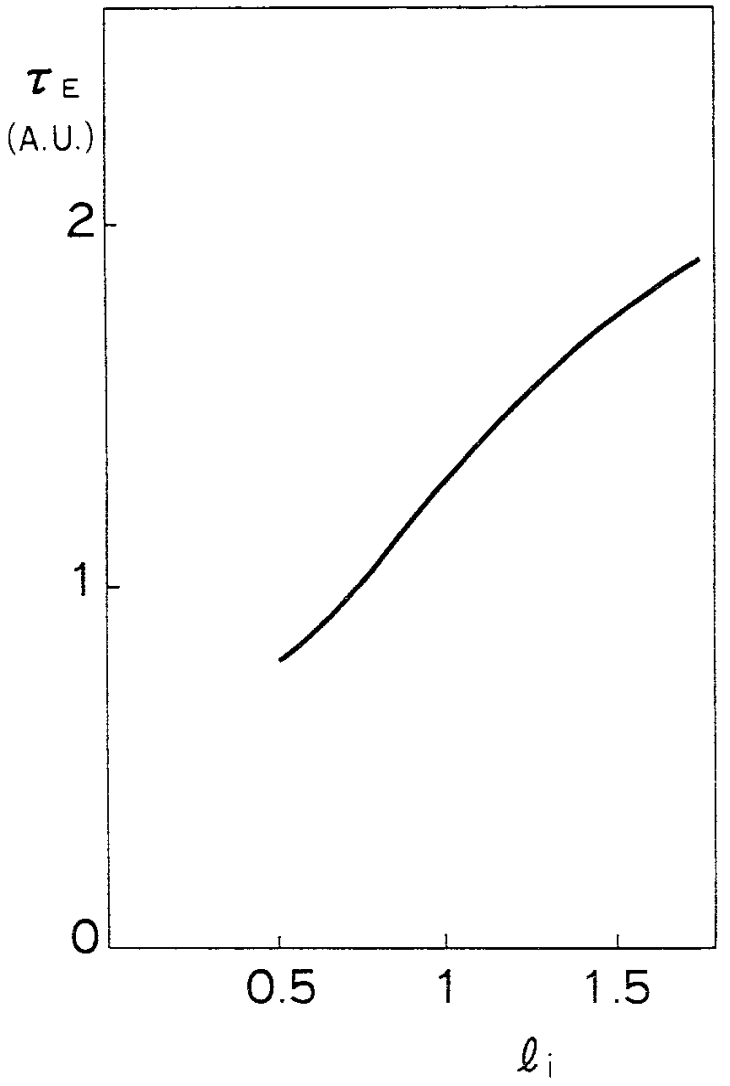

Recent Issues of NIFS Series

NIFS-175 S. -I. Itoh, K. Itoh and A. Fukuyama, *Modelling of ELMs and Dynamic Responses of the H-Mode* ; Sep. 1992

NIFS-176 K. Itoh, S.-I. Itoh, A. Fukuyama, H. Sanuki, K. Ichiguchi and J. Todoroki, *Improved Models of β-Limit, Anomalous Transport and Radial Electric Field with Loss Cone Loss in Heliotron / Torsatron* ; Sep. 1992

NIFS-177 N. Ohyabu, K. Yamazaki, I. Katanuma, H. Ji, T. Watanabe, K. Watanabe, H. Akao, K. Akaishi, T. Ono, H. Kaneko, T. Kawamura, Y. Kubota, N. Noda, A. Sagara, O. Motojima, M. Fujiwara and A. Iiyoshi, *Design Study of LHD Helical Divertor and High Temperature Divertor Plasma Operation* ; Sep. 1992

NIFS-178 H. Sanuki, K. Itoh and S.-I. Itoh, *Selfconsistent Analysis of Radial Electric Field and Fast Ion Losses in CHS Torsatron / Heliotron* ; Sep. 1992

NIFS-179 K. Toi, S. Morita, K. Kawahata, K. Ida, T. Watari, R. Kumazawa, A. Ando, Y. Oka, K. Ohkubo, Y. Hamada, K. Adati, R. Akiyama, S. Hidekuma, S. Hirokura, O. Kaneko, T. Kawamoto, Y. Kawasumi, M. Kojima, T. Kuroda, K. Masai, K. Narihara, Y. Ogawa, S. Okajima, M. Sakamoto, M. Sasao, K. Sato, K. N. Sato, T. Seki, F. Shimpo, S. Tanahashi, Y. Taniguchi, T. Tsuzuki, *New Features of L-H Transition in Limiter H-Modes of JIPP T-IIU* ; Sep. 1992

NIFS-180 H. Momota, Y. Tomita, A. Ishida, Y. Kohzaki, M. Ohnishi, S. Ohi, Y. Nakao and M. Nishikawa, *D-^{3}He Fueled FRC Reactor "Artemis-L"* ; Sep. 1992

NIFS-181 T. Watari, R. Kumazawa, T. Seki, Y. Yasaka, A. Ando, Y. Oka,O. Kaneko, K. Adati, R. Akiyama, Y. Hamada, S. Hidekuma, S. Hirokura, K. Ida, K. Kawahata, T. Kawamoto, Y. Kawasumi, S. Kitagawa, M. Kojima, T. Kuroda, K. Masai, S. Morita, K. Narihara, Y. Ogawa, K. Ohkubo, S. Okajima, T. Ozaki, M. Sakamoto, M. Sasao, K. Sato, K. N. Sato, F.Shimpo, H. Takahashi, S. Tanahasi, Y. Taniguchi, K. Toi, T. Tsuzuki and M. Ono, *The New Features of Ion Bernstein Wave Heating in JIPP T-IIU Tokamak* ;Sep, 1992

NIFS-182 K. Itoh, H. Sanuki and S.-I. Itoh, *Effect of Alpha Particles on Radial Electric Field Structure in Torsatron / Heliotron Reactor*; Sep. 1992

NIFS-183 S. Morimoto, M. Sato, H. Yamada, H. Ji, S. Okamura, S. Kubo, O. Motojima, M. Murakami, T. C. Jernigan, T. S. Bigelow, A. C. England, R. S. Isler, J. F. Lyon, C. H. Ma, D. A. Rasmussen, C. R. Schaich, J. B. Wilgen and J. L. Yarber, *Long Pulse Discharges*

Sustained by Second Harmonic Electron Cyclotron Heating Using a 35GH$_Z$ Gyrotron in the Advanced Toroidal Facility; Sep. 1992

NIFS-184 S. Okamura, K. Hanatani, K. Nishimura, R. Akiyama, T. Amano, H. Arimoto, M. Fujiwara, M. Hosokawa, K. Ida, H. Idei, H. Iguchi, O. Kaneko, T. Kawamoto, S. Kubo, R. Kumazawa, K. Matsuoka, S. Morita, O. Motojima, T. Mutoh, N. Nakajima, N. Noda, M. Okamoto, T. Ozaki, A. Sagara, S. Sakakibara, H. Sanuki, T. Seki, T. Shoji, F. Shimbo, C. Takahashi, Y. Takeiri, Y. Takita, K. Toi, K. Tsumori, M. Ueda, T. Watari, H. Yamada and I. Yamada, *Heating Experiments Using Neutral Beams with Variable Injection Angle and ICRF Waves in CHS* ; Sep. 1992

NIFS-185 H. Yamada, S. Morita, K. Ida, S. Okamura, H. Iguchi, S. Sakakibara, K. Nishimura, R. Akiyama, H. Arimoto, M. Fujiwara, K. Hanatani, S. P. Hirshman, K. Ichiguchi, H. Idei, O. Kaneko, T. Kawamoto, S. Kubo, D. K. Lee, K. Matsuoka, O, Motojima, T. Ozaki, V. D. Pustovitov, A. Sagara, H. Sanuki, T. Shoji, C. Takahashi, Y. Takeiri, Y. Takita, S. Tanahashi, J. Todoroki, K. Toi, K. Tsumori, M. Ueda and I. Yamada, *MHD and Confinement Characteristics in the High-β Regime on the CHS Low-Aspect-Ratio Heliotron / Torsatron* ; Sep. 1992

NIFS-186 S. Morita, H. Yamada, H. Iguchi, K. Adati, R. Akiyama, H. Arimoto, M. Fujiwara, Y. Hamada, K. Ida, H. Idei, O. Kaneko, K. Kawahata, T. Kawamoto, S. Kubo, R. Kumazawa, K. Matsuoka, T. Morisaki, K. Nishimura, S. Okamura, T. Ozaki, T. Seki, M. Sakurai, S, Sakakibara, A. Sagara, C. Takahashi, Y. Takeiri, H. Takenaga, Y. Takita, K. Toi, K. Tsumori, K. Uchino, M. Ueda, T. Watari, I. Yamada, *A Role of Neutral Hydrogen in CHS Plasmas with Reheat and Collapse and Comparison with JIPP T-IIU Tokamak Plasmas* ; Sep. 1992

NIFS-187 K. Ioth, S.-I. Itoh, A. Fukuyama, M. Yagi and M. Azumi, *Model of the L-Mode Confinement in Tokamaks* ; Sep. 1992

NIFS-188 K. Itoh, A. Fukuyama and S.-I. Itoh, *Beta-Limiting Phenomena in High-Aspect-Ratio Toroidal Helical Plasmas*; Oct. 1992

NIFS-189 K. Itoh, S. -I. Itoh and A. Fukuyama, *Cross Field Ion Motion at Sawtooth Crash* ; Oct. 1992

NIFS-190 N. Noda, Y. Kubota, A. Sagara, N. Ohyabu, K. Akaishi, H. Ji, O. Motojima, M. Hashiba, I. Fujita, T. Hino, T. Yamashina, T. Matsuda, T. Sogabe, T. Matsumoto, K. Kuroda, S. Yamazaki, H. Ise, J. Adachi and T. Suzuki, *Design Study on Divertor Plates of Large Helical Device (LHD)* ; Oct. 1992

NIFS-191 Y. Kondoh, Y. Hosaka and K. Ishii, *Kernel Optimum Nearly-Analytical*

Discretization (KOND) Algorithm Applied to Parabolic and Hyperbolic Equations : Oct. 1992

NIFS-192 K. Itoh, M. Yagi, S.-I. Itoh, A. Fukuyama and M. Azumi, *L-Mode Confinement Model Based on Transport-MHD Theory in Tokamaks* ; Oct. 1992

NIFS-193 T. Watari, *Review of Japanese Results on Heating and Current Drive* ; Oct. 1992

NIFS-194 Y. Kondoh, *Eigenfunction for Dissipative Dynamics Operator and Attractor of Dissipative Structure* ; Oct. 1992

NIFS-195 T. Watanabe, H. Oya, K. Watanabe and T. Sato, *Comprehensive Simulation Study on Local and Global Development of Auroral Arcs and Field-Aligned Potentials* ; Oct. 1992

NIFS-196 T. Mori, K. Akaishi, Y. Kubota, O. Motojima, M. Mushiaki, Y. Funato and Y. Hanaoka, *Pumping Experiment of Water on B and LaB_6 Films with Electron Beam Evaporator* ; Oct., 1992

NIFS-197 T. Kato and K. Masai, *X-ray Spectra from Hinotori Satellite and Suprathermal Electrons* ; Oct. 1992

NIFS-198 K. Toi, S. Okamura, H. Iguchi, H. Yamada, S. Morita, S. Sakakibara, K. Ida, K. Nishimura, K. Matsuoka, R. Akiyama, H. Arimoto, M. Fujiwara, M. Hosokawa, H. Idei, O. Kaneko, S. Kubo, A. Sagara, C. Takahashi, Y. Takeiri, Y. Takita, K. Tsumori, I. Yamada and H. Zushi, *Formation of H-mode Like Transport Barrier in the CHS Heliotron / Torsatron* ; Oct. 1992

NIFS-199 M. Tanaka, *A Kinetic Simulation of Low-Frequency Electromagnetic Phenomena in Inhomogeneous Plasmas of Three-Dimensions* ; Nov. 1992

NIFS-200 K. Itoh, S.-I. Itoh, H. Sanuki and A. Fukuyama, *Roles of Electric Field on Toroidal Magnetic Confinement*, Nov. 1992

NIFS-201 G. Gnudi and T. Hatori, *Hamiltonian for the Toroidal Helical Magnetic Field Lines in the Vacuum*; Nov. 1992

NIFS-202 K. Itoh, S.-I. Itoh and A. Fukuyama, *Physics of Transport Phenomena in Magnetic Confinement Plasmas*; Dec. 1992

NIFS-203 Y. Hamada, Y. Kawasumi, H. Iguchi, A. Fujisawa, Y. Abe and M. Takahashi, *Mesh Effect in a Parallel Plate Analyzer*; Dec. 1992

NIFS-204 T. Okada and H. Tazawa, *Two-Stream Instability for a Light Ion Beam*

-Plasma System with External Magnetic Field; Dec. 1992

NIFS-205 M. Osakabe, S. Itoh, Y. Gotoh, M. Sasao and J. Fujita, *A Compact Neutron Counter Telescope with Thick Radiator (Cotetra) for Fusion Experiment*; Jan. 1993

NIFS-206 T. Yabe and F. Xiao, *Tracking Sharp Interface of Two Fluids by the CIP (Cubic-Interpolated Propagation) Scheme*, Jan. 1993

NIFS-207 A. Kageyama, K. Watanabe and T. Sato, *Simulation Study of MHD Dynamo : Convection in a Rotating Spherical Shell*; Feb. 1993

NIFS-208 M. Okamoto and S. Murakami, *Plasma Heating in Toroidal Systems*; Feb. 1993

NIFS-209 K. Masai, *Density Dependence of Line Intensities and Application to Plasma Diagnostics*; Feb. 1993

NIFS-210 K. Ohkubo, M. Hosokawa, S. Kubo, M. Sato, Y. Takita and T. Kuroda, *R&D of Transmission Lines for ECH System* ; Feb. 1993

NIFS-211 A. A. Shishkin, K. Y. Watanabe, K. Yamazaki, O. Motojima, D. L. Grekov, M. S. Smirnova and A. V. Zolotukhin, *Some Features of Particle Orbit Behavior in LHD Configurations*; Mar. 1993

NIFS-212 Y. Kondoh, Y. Hosaka and J.-L. Liang, *Demonstration for Novel Self-organization Theory by Three-Dimensional Magnetohydrodynamic Simulation*; Mar. 1993

NIFS-213 K. Itoh, H. Sanuki and S.-I. Itoh, *Thermal and Electric Oscillation Driven by Orbit Loss in Helical Systems*; Mar. 1993

NIFS-214 T. Yamagishi, *Effect of Continuous Eigenvalue Spectrum on Plasma Transport in Toroidal Systems*; Mar. 1993

NIFS-215 K. Ida, K. Itoh, S.-I.Itoh, Y. Miura, JFT-2M Group and A. Fukuyama, *Thickness of the Layer of Strong Radial Electric Field in JFT-2M H-mode Plasmas*; Apr. 1993

NIFS-216 M. Yagi, K. Itoh, S.-I. Itoh, A. Fukuyama and M. Azumi, *Analysis of Current Diffusive Ballooning Mode*; Apr. 1993

NIFS-217 J. Guasp, K. Yamazaki and O. Motojima, *Particle Orbit Analysis for LHD Helical Axis Configurations* ; Apr. 1993

NIFS-218 T. Yabe, T. Ito and M. Okazaki, *Holography Machine HORN-1 for Computer-aided Retrieve of Virtual Three-dimensional Image* ; Apr. 1993